

Review

Fluorescent Probes for Biomacromolecules Based on Monomethine Cyanine Dyes

Pavel G. Pronkin  and Alexander S. Tatikolov * 

N.M. Emanuel Institute of Biochemical Physics, Russian Academy of Sciences, 119334 Moscow, Russia; pronkinp@gmail.com

* Correspondence: tatikolov@mail.ru

Abstract: Monomethine cyanine dyes (MCDs) are widely applied as biomolecular probes and stains in biochemical and biomedical research. This is based on the ability of MCDs to associate with biomolecules (mostly nucleic acids) with significant fluorescent growth. The present review considers the works devoted to the properties of MCDs and the influence of noncovalent interactions with biomacromolecules on their properties, as well as their use as noncovalent probes and stains for various biomacromolecules. The synthesis and photonics (photophysics and photochemistry; in particular, the generation of the triplet state) of MCDs are also considered. Areas and prospects of the practical applications of MCDs in biochemistry and biomedicine are discussed.

Keywords: monomethine cyanine dyes; nucleic acids; proteins; fluorescent probes; spectral-fluorescent properties; aggregates; noncovalent interactions; photonics

1. Introduction

Spectral-fluorescent detection and quantification of biomacromolecules is used in various biochemical and biomedical studies. It is widely applied in modern techniques such as real-time PCR, gel electrophoresis, flow cytometry, blotting, etc. This method is based on the ability of some fluorescent dyes (probes) to associate with target biomolecules with significant changes in spectral-fluorescent characteristics. Polymethine (cyanine) dyes can serve as such probes due to their unique properties, including, first of all, their high extinction coefficients, moderate fluorescence, and the dependence of the spectral-fluorescent properties on the molecular environment. Additionally, notable is the ability of cyanines to form ordered aggregates: dimers and H- and J-aggregates [1]. An important prerequisite for the use of cyanine dyes as probes is that they can bind noncovalently to various biomacromolecules, which is usually accompanied by a fluorescent growth [2,3]. Cyanine dyes contain the cyanine chromophore, which is a polymethine chain with conjugated $-C=C-$ bonds that typically connect N-containing end heterocycles and has an odd number of carbon atoms. The length of this chain largely influences the dye's spectral range of emission and absorption. Cyanines typically have a chromophore moiety with a total positive charge [3]. Monomethine cyanine dyes (MCD) represent a class of cyanine dyes with the shortest polymethine chain, which consists of only one $-CH=$ unit linking terminal heterocyclic groups. They can be both symmetrical and unsymmetrical (Figure 1). For simplicity, counterions in the structures of dyes are not shown.

Although the first MCD was synthesized by C.G. Williams back in 1856 [4], MCDs have been widely used only since the early 1990s due to their application as nucleic acid probes and labels. The MCD first used as such a probe (in reticulocyte analysis) was the unsymmetrical dye thiazole orange (TO; 1; Figure 1) [5].

At present, MCDs (mostly unsymmetrical, both monomers and covalent dimers) are very numerous, due to their wide use as nucleic acid probes and stains. Among the cyanines, they are the best nucleic acid labels with very high fluorescent growth.



Citation: Pronkin, P.G.; Tatikolov, A.S. Fluorescent Probes for Biomacromolecules Based on Monomethine Cyanine Dyes. *Chemosensors* **2023**, *11*, 280. <https://doi.org/10.3390/chemosensors11050280>

Academic Editor: Zhiyi Yao

Received: 3 April 2023

Revised: 24 April 2023

Accepted: 5 May 2023

Published: 7 May 2023



Copyright: © 2023 by the authors. Licensee MDPI, Basel, Switzerland. This article is an open access article distributed under the terms and conditions of the Creative Commons Attribution (CC BY) license (<https://creativecommons.org/licenses/by/4.0/>).

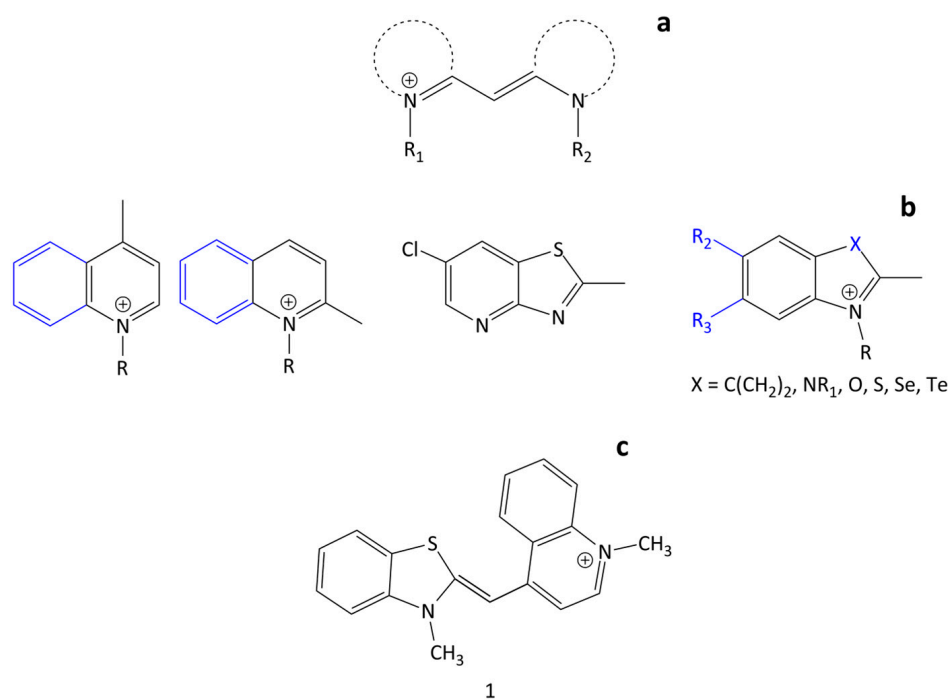


Figure 1. General structure of monomethine cyanine dyes (a) with some examples of terminal heterocyclic groups (b); structure of dye 1 (c).

This review considers the works devoted to the properties of MCDs and their use as noncovalent probes and stains for various biomacromolecules. The synthesis and photonics (photophysics and photochemistry) of MCDs and the influence of noncovalent interactions with biomacromolecules on their properties are also considered. Areas and prospects of the practical applications of MCDs are discussed.

2. Synthesis of MCDs

The methods of synthesis of MCDs of various structures (both symmetrical and unsymmetrical) were described in [6]. These include the nitrite method (using an ester or salt of nitrous acid); the alkyl- or aryl-thio method; condensations based on reactive =N-R; 4'-cyanine condensation involving the elimination of HX + H₂; Y-cyanine condensation involving reactive I, Cl, CN, or SO₃R; elimination of 2HX; and other methods. The syntheses of MCDs with substituents in the polymethine chain were also described.

Some noticeable examples of the syntheses are presented below.

The well-known thioalkyl method for the synthesis of MCDs with benzothiazole nuclei was used in [7]. This was a condensation reaction of a 2-thiomethylbenzothiazolium salt with another alkylated heterocycle having an activated methyl group (Figure 2).

This method was used in a recent work [8] for the synthesis of symmetrical MCDs with various terminal heterocyclic groups and substituents at nitrogen atoms. It is also widely used for the synthesis of unsymmetrical MCDs with different heterocyclic residues [9–12]. The thioalkyl method was applied in the synthesis of a number of MCDs derived from SYBR green II [13].

In [14], a new modification of this method was proposed for the synthesis of uncharged monomethine cyanine dyes. The authors suggest avoiding the use of two quaternary precursors, which reduces the number of steps. Monocationic and dicationic MCDs of the TO family were prepared by the thioalkyl method under solvent-free microwave irradiation by condensation of benzothiazolium salts with quaternary quinolone salts having a reactive methyl group in the presence of triethylamine [15].

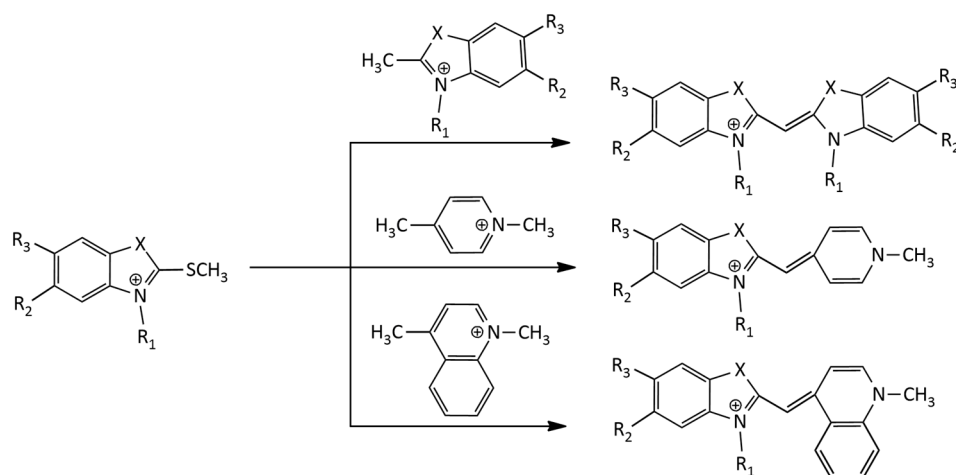


Figure 2. Scheme of the thioalkyl method for the synthesis of MCDs.

The formation of toxic methyl mercaptan is a significant disadvantage of the method. Another disadvantage is that the alkyl groups at sulfur and nitrogen atoms in the starting compounds can change their positions, which leads to an appearance of byproducts of the reaction. This disadvantage is absent in the synthesis of MCDs via melting 2-iminobenzothiazoline with a quaternary heterocyclic salt containing a 2- or 4-methyl group [16]. This method has been successfully applied to the synthesis of both symmetrical and unsymmetrical MCDs (Figure 3):

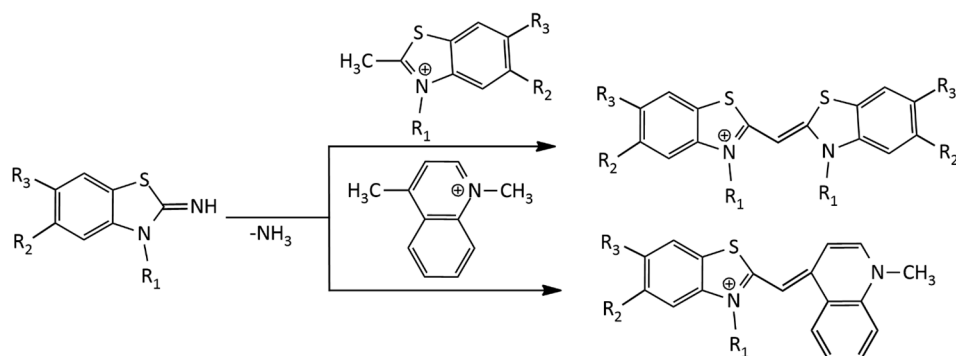


Figure 3. Scheme of the 2-iminobenzothiazoline method for the synthesis of MCDs.

Another procedure for the synthesis of MCDs, using a sulfobetaine salt of the N-alkyl heterocycle and a quaternary heterocyclic compound containing a reactive methylene group (Figure 4), was also proposed [17].

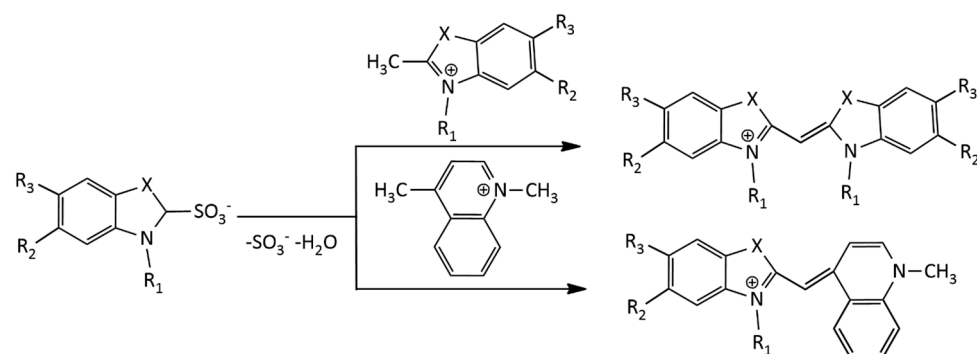


Figure 4. Scheme of the synthesis of MCDs via a sulfobetaine salt of the N-alkyl heterocycle.

An alternative method (Figure 5) was applied to the synthesis of dicationic and tricationic MCDs (benzothiazole derivatives) via condensation in a basic medium of an N-alkyl-2-methylbenzothiazolium salt with a 2- or 4-chloroquinoline derivative [18]. In [19], the synthesis of monocationic MCDs was carried out via condensation of quaternized salts of 2-ethylbenzothiazole and 4-chloroquinolinium in the presence of N-ethyldiisopropylamine.

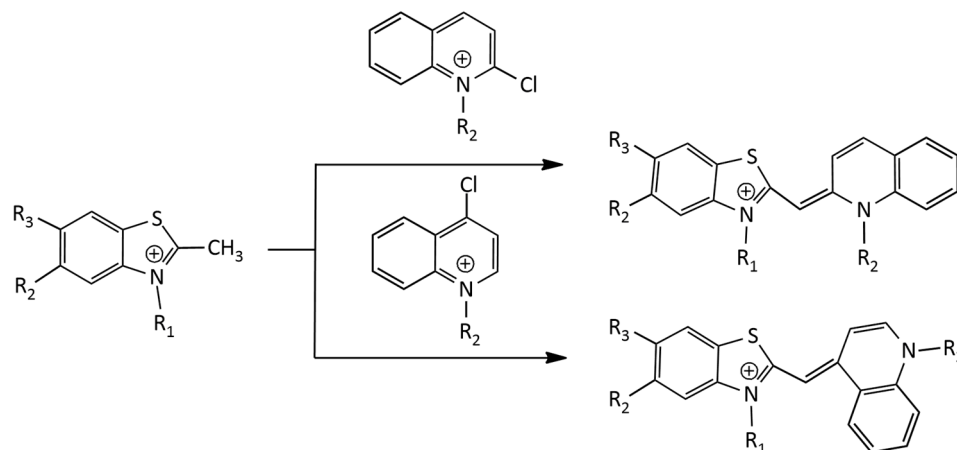


Figure 5. Scheme of MCD synthesis via 2- or 4-chloroquinoline derivative.

In particular, in the work [20], a number of tricationic analogues of TO were obtained (see Figure 5), having as substituents R_1 and R_2 (additional cationic groups) trimethylammonium, triethylammonium, 1-methylpyrrolidinium, 4-methylmorpholinium, pyridinium, N,N-dimethylpyridinium, and 3-(dimethylammonio)propan-1-ol. The works [19,21] describe the synthesis and properties of a number of monocationic, dicationic and tricationic MCDs of the TO family, the molecules of which contain carbamoylethyl, 2-hydroxypropyl, and 3-chloro-2-hydroxypropyl substituents.

The synthesis of unsymmetrical neutral pH-sensitive a MCD based on 3-phenyl-2H-1,4-benzothiazine via its condensation with indole-3-carboxaldehyde was described (Figure 6; dye yield, ~50%) [22]:

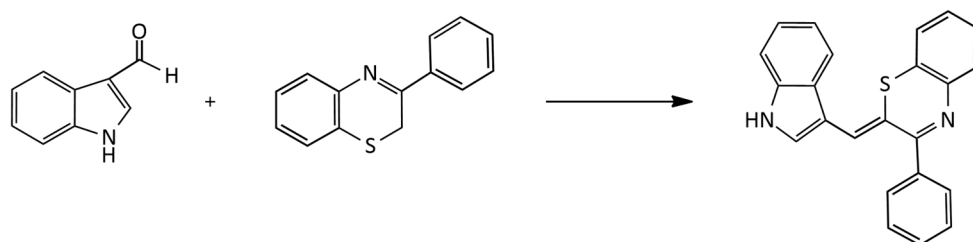


Figure 6. Scheme of the synthesis of unsymmetrical neutral pH-sensitive MCDs.

Grinding at room temperature with a small amount of a catalyst was used to synthesize a MCD in a solvent-free, effective, and environmentally friendly manner (Figure 7) [23]. The method's benefits include the mild conditions, good conversion, and low procedure costs.

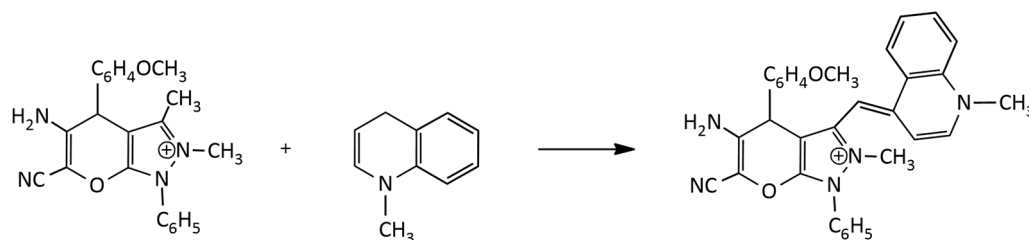


Figure 7. New, green and solvent-free synthesis of unsymmetrical MCDs.

In [24] a new efficient procedure for the synthesis of MCDs (TO and its derivatives) was proposed by the method of traceless cleavage of the Merrifield resin. The cleavage of the Merrifield resin was carried out during the solid-phase synthesis of a dye. An important advantage of the synthesis is the elimination of the long-term purification step characteristic of the traditional liquid-phase method, which makes it possible to use the synthesized dyes directly for biological purposes.

For the synthesis of homodimeric MCDs having 4 positive charges, the following scheme is known (Figure 8) [25]:

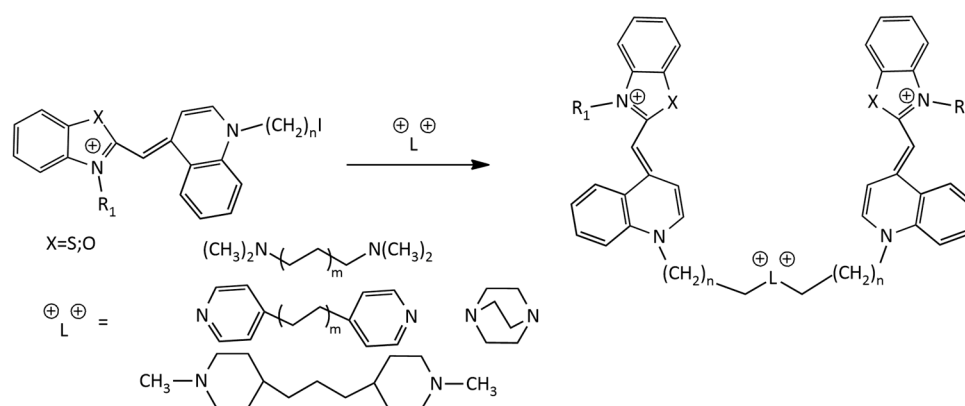


Figure 8. Scheme of the synthesis of homodimeric MCDs.

In [26] the synthesis of new dimeric MCDs based on the TO chromophore under the action of microwave radiation was described. The synthesis is performed via the reaction of a monomethine dye having an iodoalkyl group with tertiary diamine linkers. In [27], the synthesis of homodimeric derivatives of dye 1 (TO) with various linkers was described (Figure 8).

Details of the methods of MCD synthesis are summarized in Table 1.

Table 1. Details of the methods of MCD synthesis.

Reaction Scheme	Precursor Compound	Reagents/Solvents, Conditions	Temperature, Time	Reaction Yield	Refs.
Figure 2	Thioalkyl derivatives	Dry pyridine or triethylamine in ethanol	120 °C	68–94%	[8]
		N-diisopropylethylamine in ethanol or acetic anhydride	Room temperature	34–98%	[9]
		Trimethylamine in acetonitrile	60 °C	34–90%	[10]
		N,N-Diisopropylethylamine in methanol, with diethyl ether added	Room temperature	21–63%	[11,12]
		Triethylamine, dichloromethane	Room temperature	10–37%	[13]
Figure 3	2-iminobenzothiazoline	Melting of compounds, then cooling, and ethanol addition	100–110 °C (10–15 min)	52–95%	[14]
		Triethylamine, solvent-free, microwave	260–320 W, 5–8 min; 200–240 W, 10–12 min ¹	75–93%; 79–90% ¹	[15]
Figure 4	Sulfobetaine salt of N-alkyl heterocycle	Melting of compounds and addition of solvent	150–220 °C, 1 h	31–86%	[16]
Figure 5	2- or 4-chloroquinoline derivative	Melting of compounds, then cooling, and addition of methanol	100–250 °C, several min	65–95%	[17]
		Methoxyethanol, 1-methyl-2-pyrrolidinone-2, or mix.	Cooling, 10–120 min	51–95%	[17]
Figure 6	3-phenyl-2H-1,4-benzothiazine and indole-3-carboxaldehyde	Melting of compounds and addition of acetone	160 °C, 30 min	49–83%	[18]
		Triethylamine in methanol with addition of KI/H ₂ O	Cooling, 30 min	56–71%	[18]
		N,N-Diisopropylethylamine in methanol	Room temperature, 2–7 h	50–97%	[19]
		Triethylamine in methanol with addition of KI/H ₂ O.	Room temperature, 1–2 h	51–93%	[20,21]
Figure 6		12 M HCl/acetonitrile; 1:4 v/v	70 °C, 3 h	~50%	[22]

Table 1. Cont.

Reaction Scheme	Precursor Compound	Reagents/Solvents, Conditions	Temperature, Time	Reaction Yield	Refs.
Figure 7	Methyl-pyridinium iodide	Grinding of compounds (in the presence of piperidine catalyst) of 2-methoxyethanol, with addition of KI/H ₂ O.	Room temperature, 13 min	90–97%	[23]
Figure 8	Thiazole orange derivative ¹	Microwave-assisted solvent-free method, in the presence of N,N-dimethylformamide and triethylamine	70–120 W, 78–110 min	75–90%	[26]
		2-methoxyethanol	2–5 h	31–51%	[27]

¹ For dimeric dyes.

3. Photonics of MCD in Solution

The photonics (photophysical and photochemical properties) of MCDs were studied in a number of works. Depending of the nature of the terminal heterocycles in their molecules, the absorption spectral maxima of MCDs range from ~420 to >600 nm, with extinction coefficients of up to $10^5 \text{ M}^{-1} \text{ cm}^{-1}$. Fluorescence quantum yields of MCDs in nonviscous solvents are usually very low [10]; for example, for 1,1'-diethyl-2,2'-cyanine (2, Figure 9; pseudoisocyanine, PIC) in ethanol, the Φ_f was estimated to be ~0.1% [28]. This is explained by the ultrafast nonradiative deactivation of the excited state (S_1) of MCDs.

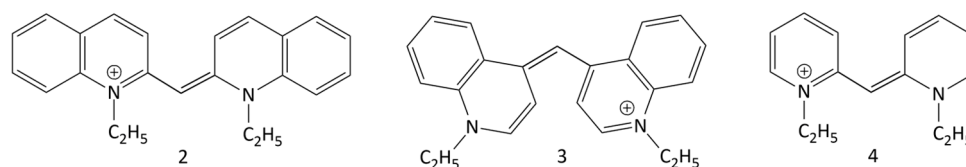


Figure 9. Structural formulas of symmetrical “simplest” MCDs 2–4. The compound names are given in the text.

The dynamics of the S_1 state of some symmetrical MCDs (in particular, MCD 2 (PIC), 3 (1,1'-diethyl-4,4'-cyanine), and 4 (1,1'-diethyl-2,2'-pyridocyanine); see Figure 9) were studied by picosecond and femtosecond spectroscopy [29–34]. The ultrafast deactivation of the S_1 state of a MCD is explained by the barrierless character of its potential surface. The deactivation leads to rapid internal conversion ($S_1 \sim \rightarrow S_0$) and *trans-cis* isomerization via rotation around the methine bridge (Figure 10).

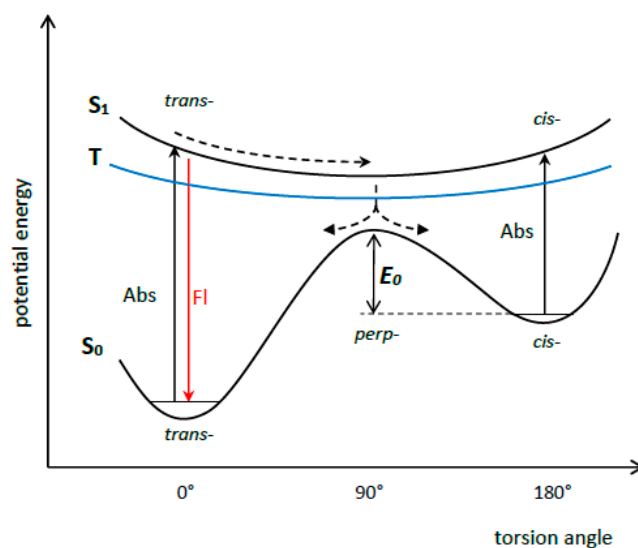


Figure 10. Scheme of potential surfaces of the S_0 , S_1 and T states of dye 2 and nonradiative deactivation of its S_1 state (based on [32]).

The excited-state dynamics of commonly used unsymmetrical dyes, derivatives of oxazole yellow (YO) (5–8; Figure 11), were studied in water using ultrafast fluorescence spectroscopy. Both the monomer and H-dimer of the dyes exhibit very weak emission; the monomer exhibits this property due to extremely fast nonradiative deactivation with a time constant of about 3–4 ps, while the H-dimer has weak emission due to excitonic coupling [35].

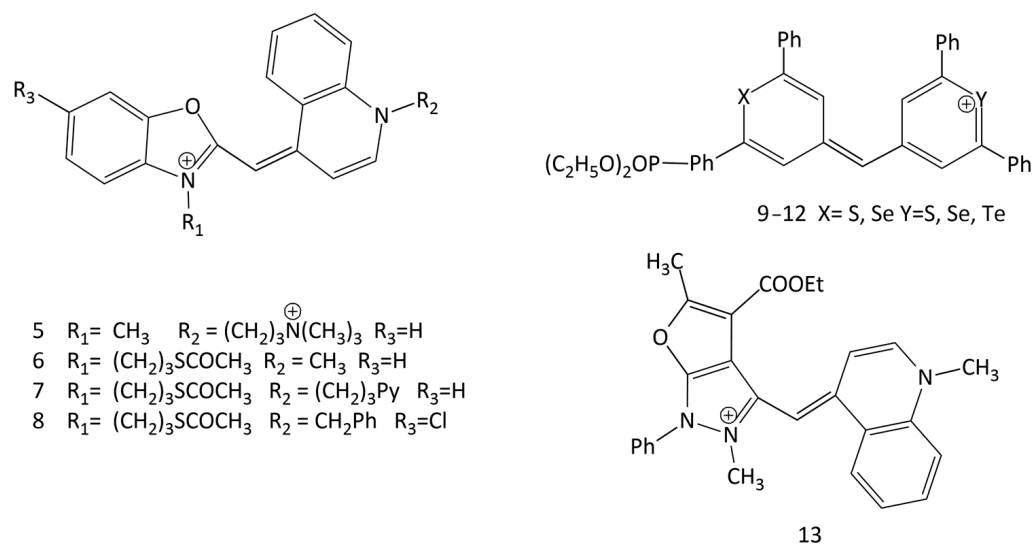


Figure 11. Structural formulas of unsymmetrical MCDs 5–13.

The ultrafast excited-state dynamics in an aqueous solution were also studied for another widely used unsymmetrical dye, MCD 1 (TO, see Figure 1) [36]. The fluorescence lifetime of 1 was found to be extremely short (~ 1 ps). This explains the very low fluorescence quantum yield of 1 in water ($\sim 0.02\%$) [37].

It has been shown that the spatial configurations of both *trans*- and *cis*-isomers of 4 are nonplanar [33]. *Trans*- and *cis*-isomers of 2 were shown to exist in solution at the same time [31]. In [38], photoisomerization of MCDs was studied theoretically. To characterize the photoisomerization of such dyes, a Hamiltonian model for the electronic structure of a monomethine dye was proposed. A valence bond structure can be associated with each of the three diabatic electronic states, and the model depicts interactions between them.

The quantum yield of intersystem crossing to the triplet state of MCDs in nonviscous solvents is usually close to zero. However, for the Te-substituted dye 12 (Figure 11; $X = \text{S}$, $Y = \text{Te}$) it reaches 10% (heavy atom effect). It also increases in viscous solvents [34].

MCD 2 is capable of forming J-aggregates in aqueous solutions (exhibiting a narrow absorption band with a maximum at ~ 573 nm) [39].

In [40], the solvatofluorochromic properties of an unusual MCD, furo [2,3-*b*]pyrazolocyanine 13 (Figure 11), were studied. Its UV-Vis spectra are characterized by the presence of two absorption bands, which is explained by intramolecular charge transfer in the cyanine molecule.

4. Interaction of MCD with DNA and Other Nucleic Acids

4.1. Monomeric MCD

Binding in the minor groove and intercalation between base pairs are the two primary types of noncovalent interactions of a cyanine dye monomer with DNA (Figure 12).

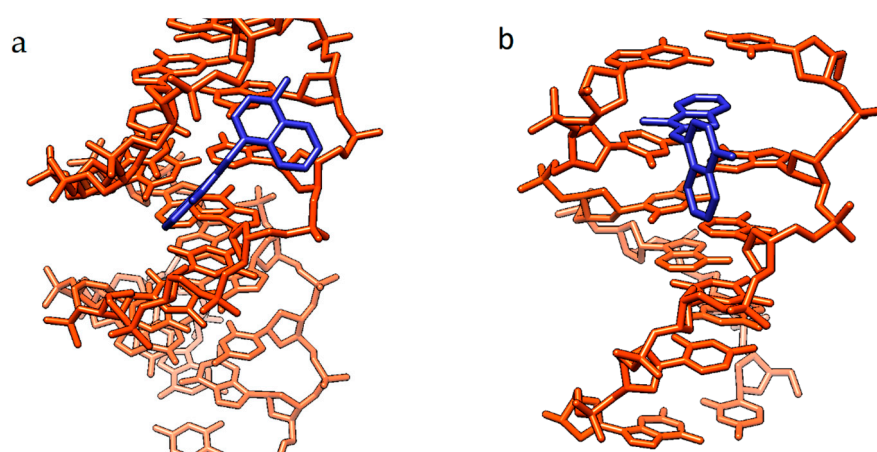


Figure 12. Conceptual scheme of noncovalent binding of MCDs to double-stranded DNA, illustrating the main types of complexes: (a) binding in the minor groove of the DNA molecule and (b) intercalation between DNA base pairs, using dye **2** (molecules in blue) as an example.

Along with the monomer interaction, the formation of dye aggregates on nucleic acid molecules is possible.

The formation of intercalation complexes is characteristic of cyanine dyes having relatively simple and compact structures with planar aromatic terminal heterocycles. This was shown, in particular, for **2**. In [41], the interaction of **2** with dsDNA was studied using spectral-fluorescent methods and via linear dichroism (LD) and circular dichroism (CD) spectroscopies. It has been shown that CD and LD measurements can be used to monitor the dye–dsDNA interaction both stoichiometrically and structurally. Dye **2** forms two types of complexes with DNA: intercalation complexes (binding of a monomeric dye, high equilibrium constants, and insensitivity to ionic strength), dimers and J-aggregates in the DNA groove (due to electrostatic interaction) [41]. For intercalation complexes, the complexation constant $K_a \sim (9 \pm 3) \times 10^5 \text{ M}^{-1}$ was obtained (with one dye binding site per every second base pair); for the complex on the surface, K_a is much lower.

Unsymmetrical MCDs are widely used as nucleic acid probes. Among the dyes of this type, excellent results were obtained for intercalative dyes TO (**1**, Figure 1) [5,36,42,43] and YO (**14**, see Figure 13) [44,45]. A feature of these dyes is their very weak intrinsic fluorescence in an aqueous solution (due to the effective dissipation of the electronic excitation energy via intramolecular twisting [36,37]), which can lead to a huge relative increase in the fluorescence intensity upon interaction with nucleic acids. In a noncovalent dye–DNA complex, nonradiative deactivation in MCD molecules is hindered, and the fluorescence quantum yields (Φ_f) increase sharply. For example, when **1** is in water, $\Phi_f = 0.02\%$; when it is in the presence of dsDNA, $\Phi_f = 11\%$ (with the binding constant $\log K_b = 5.5$); and when it is bound to single-stranded poly(dG), $\Phi_f = 39\%$ [43]. Dye **14** also binds to DNA with fluorescent growth and intercalation between DNA base pairs [44,46].

Spectral-fluorescent characteristics and interaction with dsDNA of 16 new unsymmetrical MCDs were studied in [9]. In solutions (in an unbound form), the dyes practically do not fluoresce; the interaction with dsDNA leads to an increase in the fluorescence intensity. In particular, for dyes **15–19** (see Figure 13), the relative fluorescent growth was 892, 1033, 834, 437, and 340 times, respectively. The dye association constants for the new MCD calculated using the McGhee–von Hippel model range from 2.27×10^4 to $7.58 \times 10^5 \text{ L mol}^{-1}$. The authors suggested an intercalating mechanism for the interaction of the dyes with DNA, but did not present additional results that can directly support this hypothesis.

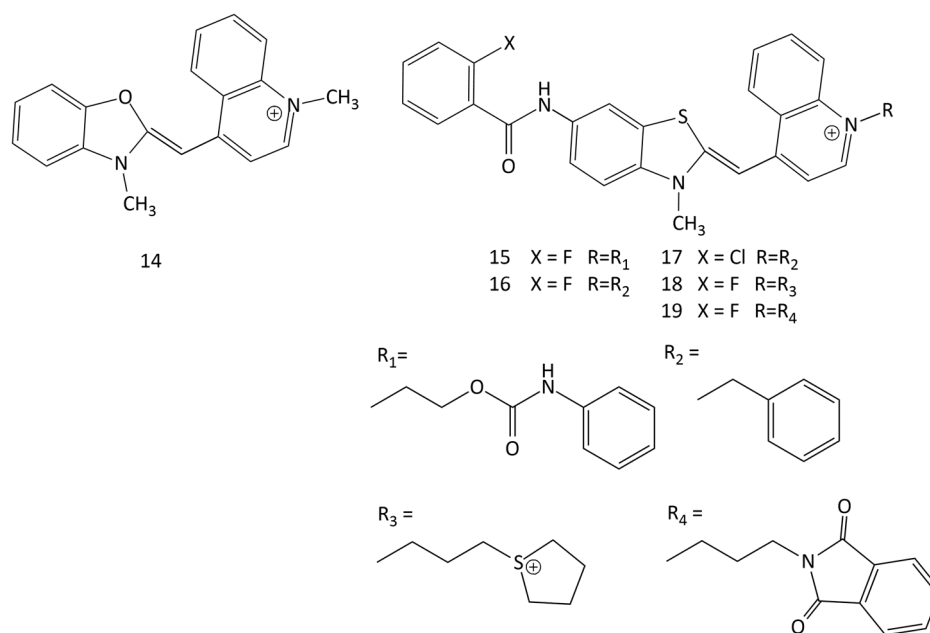


Figure 13. Structural formulas of unsymmetrical MCDs 14–19.

The interaction of new unsymmetrical MCD 20–26 (Figure 14), containing a benzoselenazole fragment, with dsDNA/RNA was studied in [11,12]. It has been shown that the dyes interact with dsDNA with significant fluorescent growth; the dyes containing a methyl group at the nitrogen atom in the benzothiazole core (dyes 20 and 21) were found to be more suitable as fluorescent markers (up to a 63-fold increase in the fluorescence intensity in the presence of dsDNA). It has been concluded that incorporation of a different heteroatom in the dye structure can lead to a multi-fold increase in the fluorescence intensity of MCDs bound to complexes with DNA. At the same time, the presence of Se atoms led to higher fluorescence intensities of the corresponding free dyes [11]. MCDs containing a Se atom have been proposed as competitive fluorescent probes for nucleic acids [11].

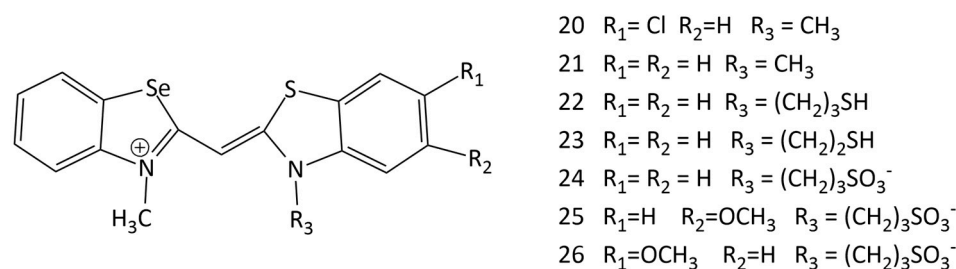


Figure 14. Structural formulas of unsymmetrical MCDs 20–26 containing a benzoselenazole heterocycle.

For ligand–biopolymer interaction, CD spectroscopy provides valuable information about the structure of the complex and the location of the ligands. Binding with DNA and RNA induces the appearance of a CD signal of initially achiral dye molecules, and various binding modes (intercalation, binding in grooves and binding of aggregated molecules on the polynucleotide backbone) cause CD signals of different intensities and signs [47,48].

The influence of various substituents in the benzothiazole nuclei of unsymmetrical MCDs containing Se on the noncovalent interaction with nucleic acids was studied via CD spectroscopy [12]. The CD spectra of compounds 20 and 21 indicated the binding of dye monomers in the minor groove of the AT DNA sequences, while GC-DNA induced bisignate signals, which indicated the aggregation of the MCDs in the grooves of the helix.

The design of substituents in the terminal nuclei of MCDs can directly affect the interaction with biomacromolecules. In [49], two guanidiniocarbonyl–pyrrole conjugates

(GCP) of MCDs were obtained (dyes **27** and **28**; Figure 15), and their interaction with nucleotides was studied. The conjugates practically do not fluoresce in solution and exhibit strong fluorescence in the presence of dsRNA and dsDNA nucleotides.

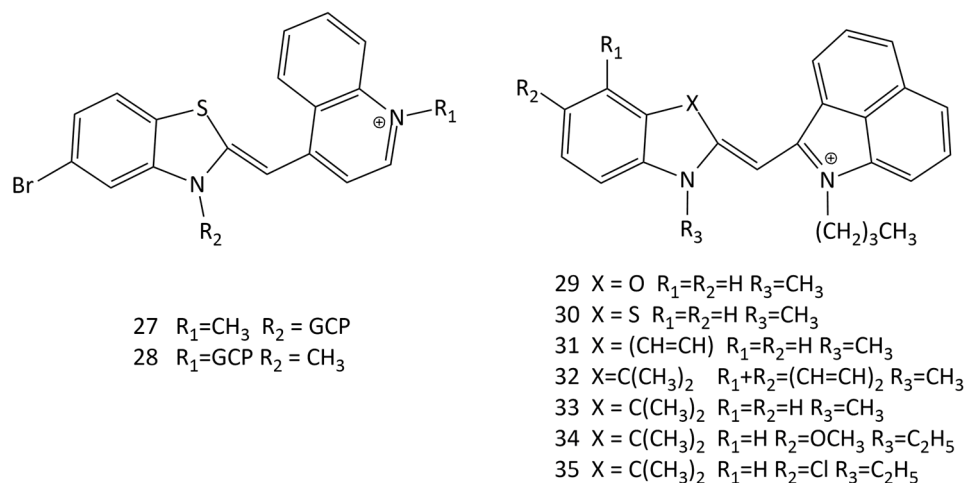


Figure 15. Structural formulas of dyes: GCP conjugates of MCDs (**27** and **28**) and unsymmetrical benz[c,d]indolium-containing MCDs (**29–35**).

In [10] the interaction of new benz[c,d]indolium-containing MCDs (see Figure 15, dyes **29–35**) with dsDNA was studied by spectral-fluorescent and molecular docking methods. The dyes were proposed as potential fluorescent probes. Docking of dye **30** showed the possibility of the formation of complexes in the small groove of the DNA double helix, and the constant of the complex formation of **30** with DNA was determined ($\sim 1 \times 10^4 \text{ L mol}^{-1}$).

The interaction of some TO-fluorinated analogues (dyes **36–39**, Figure 16) with DNA was investigated in [50]. It was shown that the presence of fluorine as a substituent significantly improves the photostability and spectral-fluorescent characteristics of the dyes.

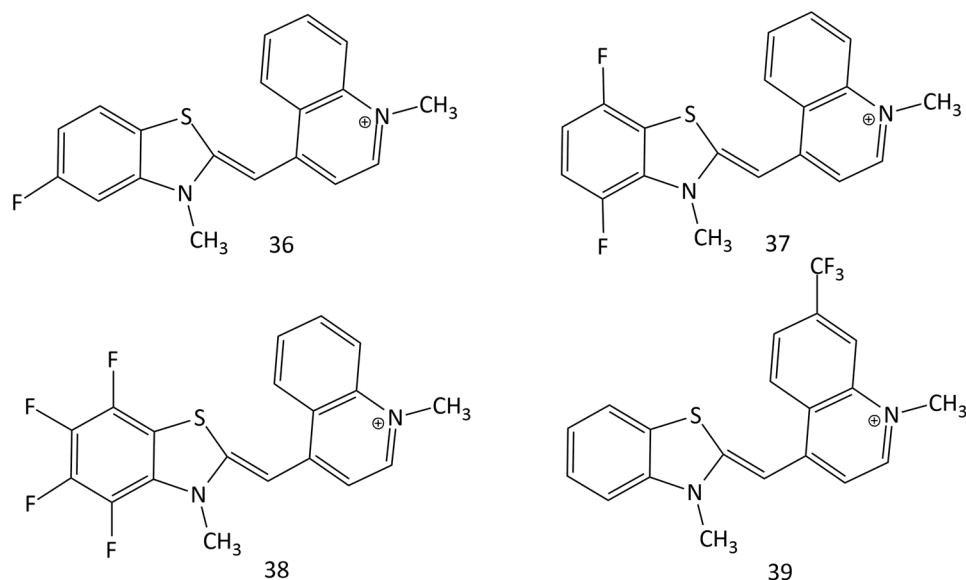


Figure 16. Structural formulas of fluorinated MCDs (dyes **36–39**).

Since Coulomb interactions play an important role in the complexation of cationic dyes with nucleic acids, an increase in the positive charge of dye molecules due to the introduction of additional cationic groups into the structure of cyanine dyes, as well as due

to the use of dimeric derivatives of cyanines, can increase their affinity for DNA and other nucleic acids.

For binding to DNA, a number of unsymmetrical MCDs with different positive charges, 40–46 (Figure 17), were synthesized and studied using spectral-fluorescent methods [51]. The dyes interact with dsDNA both via intercalation and via complexation on the surface. Some of the studied dyes are able to distinguish between single-stranded and double-stranded polynucleotides, exhibiting different fluorescence spectra. The detection limits (LOD) for most of the dyes with respect to dsDNA (for dye 40, about 70 ng/mL [51]) are comparable to those of ethidium bromide.

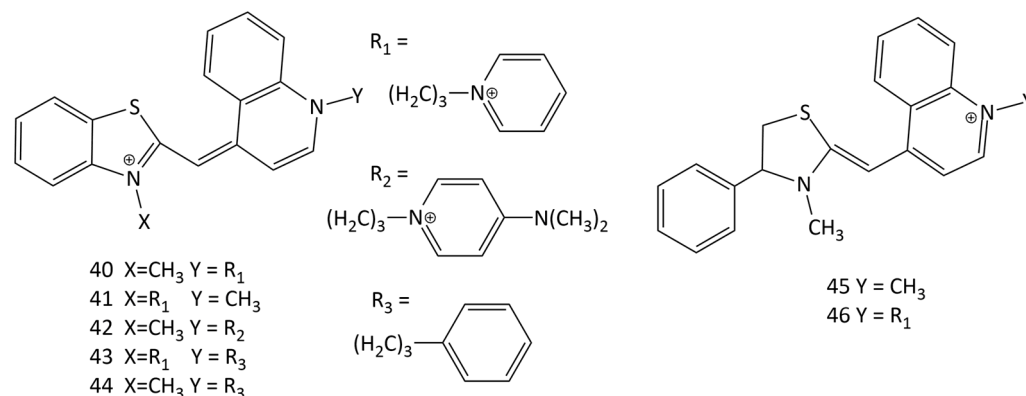


Figure 17. Unsymmetrical MCDs 40–46 with different positive charges.

Dicationic derivatives of **1**, **14**, and other MCDs with charged substituents at the N-atom of quinoline or pyridine heterocycles (**5**, **47**, **48**, **49**, and **50**; Figure 18) and their interaction with nucleic acids were thoroughly investigated [45,52–54]. For the detection of nucleic acids in solution, other analogues of **1** and **14** were synthesized and proposed (see Figure 5) [19–21,55–58].

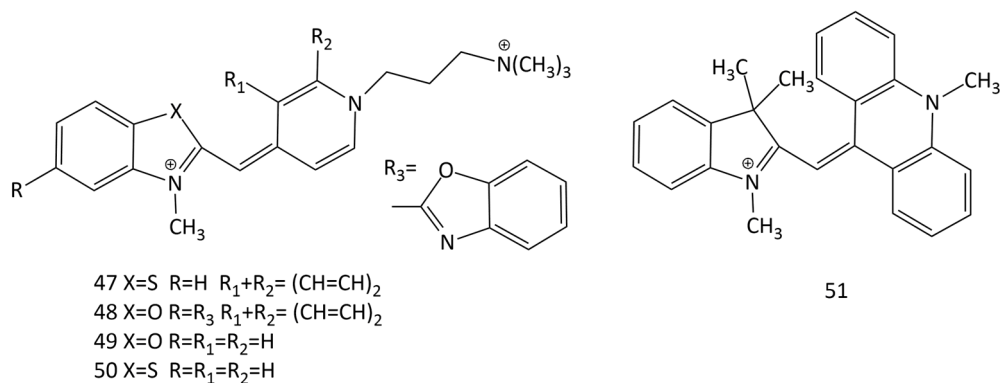


Figure 18. Structural formulas of different unsymmetrical dicationic dyes 47–50 and dye 51 with an acridine terminal heterocycle.

An unsymmetrical monomethine dye, MCD **51**, was synthesized, in which one of the terminal heterocycles was an acridinium fragment [59]. In solutions (with low viscosity), dye **51** is characterized by low fluorescence (~0.2%). Interestingly, the interaction with dsDNA leads to a decrease in the fluorescent response of dye **51**.

The interaction of a number of MCDs, derivatives of Cyan 40 (dye **52** in Figure 19), having different substituents at the N-atom in the pyridinium fragment, with nucleic acids was studied in [60] (dyes **52**–**57**; Figure 19). It was shown that the nature of the functional groups in the dye substituent affects the fluorescent properties of its complexes with DNA [60]. In [61], the equilibrium and kinetics of the binding with DNA of dye **52** were studied using the T-jump method. The binding of the dyes proceeds via the formation

of an external complex (a fast step), which, with time, is rearranged into a complex with partial intercalation, which then is converted into a completely intercalated complex [62].

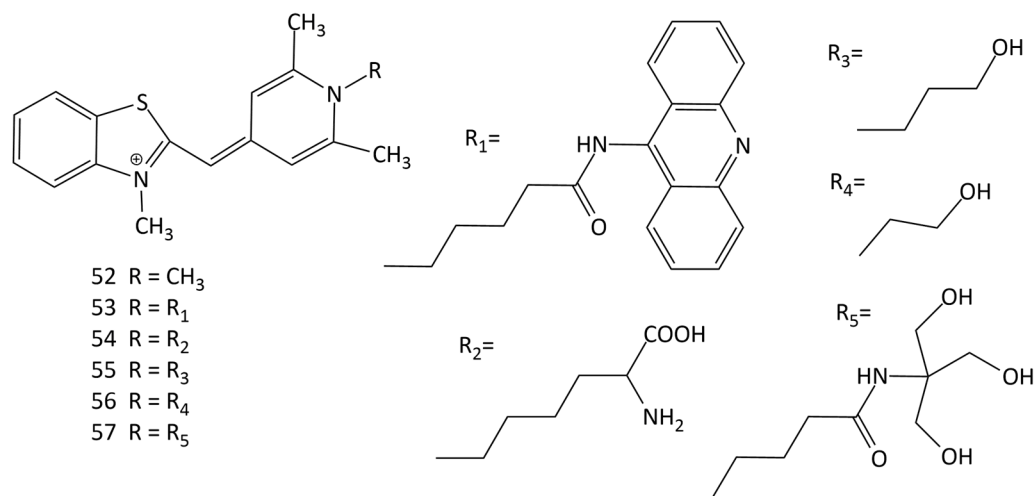


Figure 19. Structural formulas of unsymmetrical MCDs 52–57 with different substituents at the N-atom in the pyridinium fragment.

In [63], the effect of complexation with nucleic acids on the photonics of MCDs having benzothiazole heteronuclei and their analogues, as well as five monomethinepyrylium cyanines and their N-methylpyridine analogues, was studied (dyes 52 and 58–65; Figure 20). For the interaction of MCDs (in particular, dye 52) with dsDNA, a half-intercalation model was presented. According to this model, benzothiazole or benzoxazole-based terminal nuclei of MCDs intercalate, whereas pyridine or pyrylium nuclei bind in the DNA groove [63].

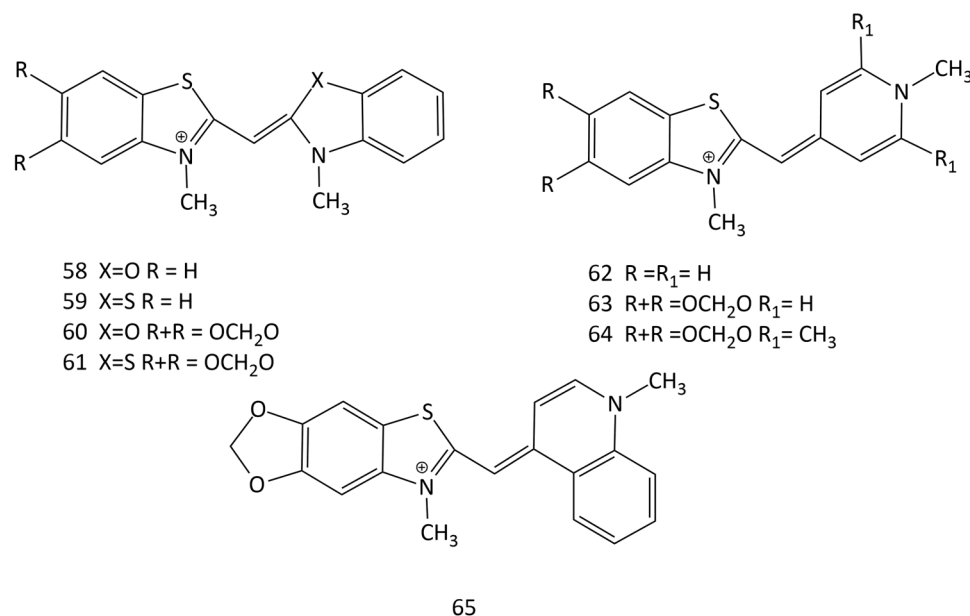


Figure 20. Structural formulas of unsymmetrical MCDs 58–65.

The work [64] describes the synthesis and properties of MCD 66 (Figure 21). Non-covalent interaction of 66 with dsDNA leads to an increase in dye emission; the MCD is proposed to replace mutagenic ethidium bromide. Note that the data on the formation of intercalation complexes by the dye and the conclusion made in this work about a one-step scheme of the MCD–DNA reaction leading to the formation of one type of monomeric dye complex require additional verification.

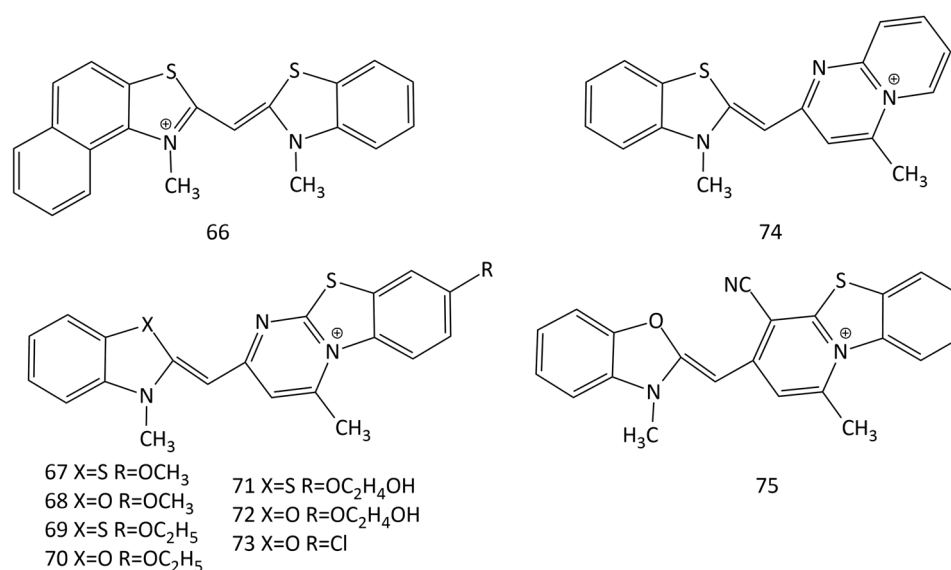


Figure 21. Structural formulas of unsymmetrical MCD 66–75.

A number of new MCDs (67–75 in Figure 21) were synthesized and studied [65,66]. The dye absorption peaks are between 450 and 500 nm.

In solution, the dyes exhibit low emission, but some become extremely luminescent when binding to DNA. For dye 67, a good LOD was obtained toward dsDNA (100 ng of DNA).

In [66], a significant influence of substituents in terminal heteronuclei was revealed. Substituents in MCD 67–73, which increase the size of dye molecules, together with the possibility of forming H-bonds with DNA (due to the OH-groups of substituents), are favorable for minor groove binding with dsDNA. MCD 74 and 75, which are characterized by compact molecular sizes, can intercalate into dsDNA and dsRNA. The selectivity of dyes 74 and 75 for dsRNA was found.

Numerous studies on various MCD fluorophores led to the emergence of a number of commercially available nucleic acid probes (in particular, SYBR Green I, PicoGreen, SYBR Green II, and SYBR Gold; dyes 76–79, respectively, in Figure 22) [67–72].

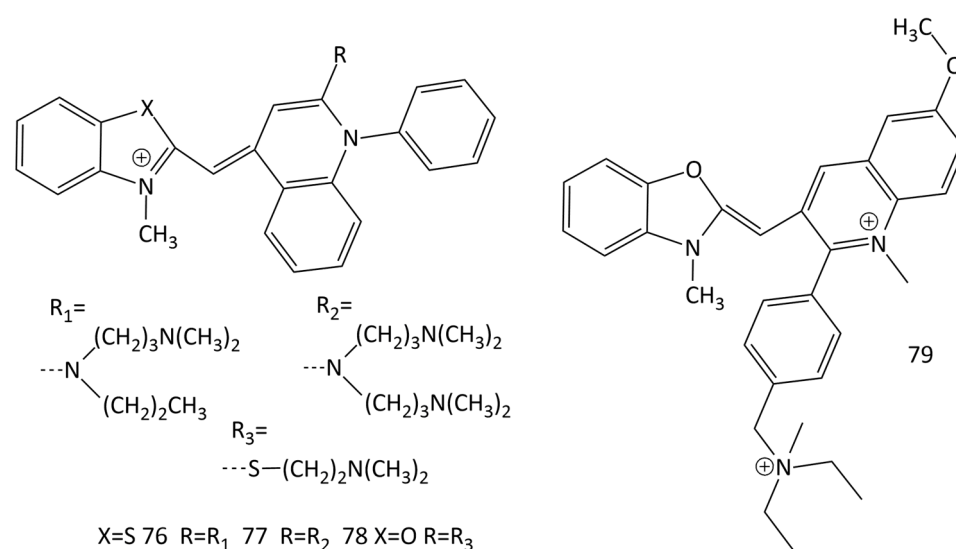


Figure 22. Structural formulas of commercially available MCDs 76–79.

It has been shown in [69] that SYBR Green I (76 in Figure 22) is capable of both intercalation between dsDNA base pairs and the formation of a highly fluorescent complex

on the surface of the double helix. Binding of SYBR Green I to ssDNA results in a significantly lower fluorescence growth (~11-fold lower than with dsDNA). In [70], using fluorescent methods and circular dichroism spectroscopy, the selectivity of PicoGreen (dye 77 in Figure 22) binding to dsDNA and ssDNA was studied in detail. It was shown that in the case of interaction of 77 with dsDNA, the intercalation complex predominates. Authors of [71] noted that the formation of intercalative complexes by dyes, as the main type of binding with dsDNA, in some cases may limit the use of such probes. The authors [73] concluded that 76 and 77 are more sensitive for detection than traditional fluorescent reporters (ethidium bromide and Hoechst 33258) are and can quantify dsDNA at concentrations of about 0.5–1 ng/mL.

In the work [74], using a set of methods (which include single-molecule magnetic tweezers (MT), NMR and mass spectrometry), the structures of MCD 79 (SYBR Gold) and 76 were determined, and their binding to DNA was studied. The experiments showed that the interaction of DNA with the dyes leads to their intercalation and is accompanied by an increase in the fluorescence intensity of the ligands. The binding constant of 76 to DNA was found (from the McGhee–von Hippel model) to be $(3.7 \pm 0.35) \times 10^6 \text{ M}^{-1}$ and the size of the binding site was $n = 1.67 \pm 0.04$ bases [74]. The structure of 78 (SYBR Green II; Figure 22) was investigated in [13].

Based on the SYBR Green I and II (76 and 78, respectively; Figure 22) chromophore, new functionalized MCDs have been developed (dyes 80–89; Figure 23) [13,75]. The design made it possible to draw some conclusions regarding the structure–property relationship, the influence of differences in heteroatoms (oxygen/sulfur) in the chromophore and substituents.

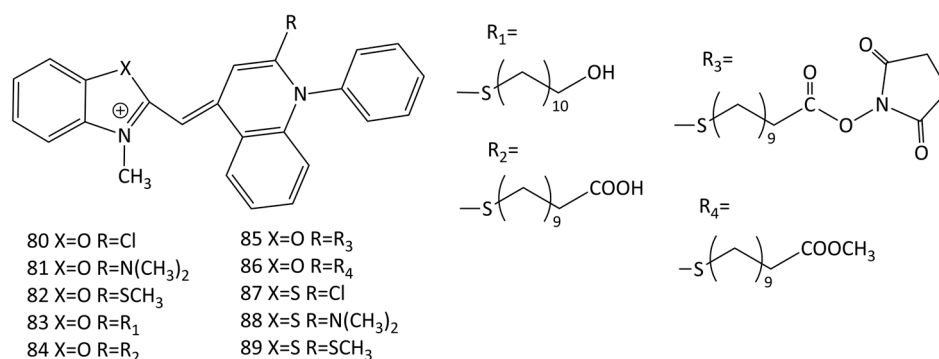


Figure 23. Structural formulas of MCDs 80–89.

Upon the interaction with calf thymus DNA, the greatest increase in the fluorescence intensity was obtained for benzoxazole dyes 81 and 82 (an increase of 11.2 and 50 times) [75]. Linear dichroism (LD) spectroscopy showed dye binding to dsDNA via intercalation [13]. The binding constants of dyes 80–89 with calf thymus DNA were $1.3\text{--}8.5 \times 10^6 \text{ M}^{-1}$ (according to the McGhee–von Hippel model), the sizes of binding sites varying slightly ($n \sim 2.2\text{--}3.4$ bases) [13,75]. The influence of substituents in heterocycles was studied; the lengthening of alkyl chains leads to the deterioration of binding (dye intercalation conditions are violated, because the sizes of nucleic acid sites increase) [13]. It was concluded [75] that the introduction of heteroatom substituents (S and Cl, dyes 82 and 89 and 80 and 87; Figure 23) into dye molecules increases photostability, but deteriorates the characteristics of the dyes as probes.

Unsymmetrical MCD molecules (90–92; Figure 24) with crescent geometries that fitted the DNA minor groove were obtained [76–79]. The aggregation of dye 92 in the presence of DNA was discussed; dyes 90–92 bind in the minor groove of the double helix. In the presence of DNA, the dyes have absorption maxima in the region of $>500 \text{ nm}$. The formation of complexes proceeds with an increase in the fluorescence intensity (14 and 50 times for 92 and 91, respectively, with a dye/DNA of ratio 1:100). Dye 91 has good potential as a probe for mixed DNA sequences.

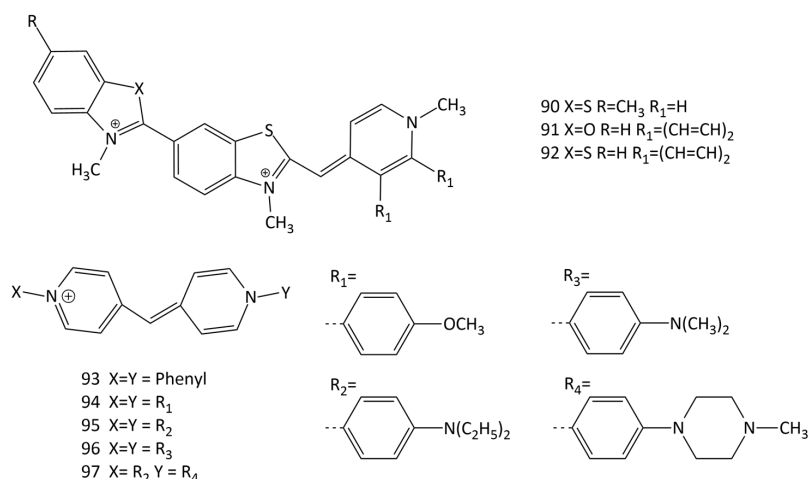


Figure 24. Structural formulas of unsymmetrical crescent-shaped MCDs (90–92) and dyes based on N-arylpyridocyanine (dyes 93–97).

The recent work [80] reports the development of MCD based on N-arylpyridocyanine (dyes 93–97; Figure 24) as DNA probes with longer-wavelength absorption (532–561 nm in the presence of DNA). It was found that N-aryl substituents not only shift the spectral maxima, but also significantly increase the efficiency of binding to DNA. CD experiments with dsDNA showed that the dyes bind in the minor groove of the double helix, which should contribute to high selectivity for DNA against RNA. In particular, the fluorescence intensity of dye 93 increased 1600 times when bound to DNA, while only a 110-fold increase was observed with RNA (selectivity 14). Dyes 95 and 96, which have diethylamino and dimethylamino groups in the para positions of the terminal nuclei, have even higher selectivity ratios (32 and 31, respectively). The highest increase in the fluorescence intensity in the presence of DNA was achieved for dye 96 (an increase of 3900 times). The experiments have shown that pyridocyanine 93 specifically binds to nucleotide AT base pairs and shares the same AATT DNA sequences with the Hoechst probe [80].

The data on the spectral-fluorescent studies of the interaction of monomeric MCD with DNA are summarized in Table 2.

Table 2. Spectral-fluorescent properties of monomeric MCD probes in the absence (f) and in the presence (b) of dsDNA. $\lambda_{\text{abs}}^{\text{f}}$ and $\lambda_{\text{fl}}^{\text{b}}$ are maxima of the absorption and fluorescence spectra, respectively; I_{fl}^{f} and I_{fl}^{b} are fluorescence intensities in the absence and in the presence of dsDNA, respectively; $\varphi_{\text{fl}}^{\text{b}}$ is the fluorescence quantum yield of the dye bound to DNA; K_{b} is the constant of dye binding to DNA; τ^{DNA} is the fluorescence lifetime in the presence of DNA; and LOQ is the limit of DNA detection (quantification).

Dye No.	Charge	$\lambda_{\text{abs}}^{\text{f}}$	$\lambda_{\text{abs}}^{\text{b}}$	$\lambda_{\text{fl}}^{\text{f}}$	$\lambda_{\text{fl}}^{\text{b}}$	$I_{\text{fl}}^{\text{b}}/I_{\text{fl}}^{\text{f}}$, $\varphi_{\text{fl}}^{\text{b}}$ (%)	K_{b} , τ^{DNA} , LOQ	Refs.
		nm						
1	+1	501	508	640	527	18900	$K_{\text{b}} = 3.2 \times 10^5 \text{ M}^{-1}$	[43,46]
14	+1	481	490	575	505	700, 36%	—	[44,46]
15	+1	508	519	—	544	892	$K_{\text{b}} = 2.3 \times 10^4 \text{ M}^{-1}$	
16	+1	501	519	—	545	1033	$K_{\text{b}} = 9.8 \times 10^4 \text{ M}^{-1}$	
17	+1	512	519	—	543	834	$K_{\text{b}} = 7.9 \times 10^4 \text{ M}^{-1}$	[9]
18	+2	510	516	—	547	437	$K_{\text{b}} = 1.27 \times 10^5 \text{ M}^{-1}$	
19	+1	512	525	—	545	340	$K_{\text{b}} = 9.8 \times 10^4 \text{ M}^{-1}$	
20	+1	426	424	495	465	7	—	
21	+1	431	433	505	480	7	—	
22	+1	423	431	491	466	63	—	
23	+1	427	436	497	470	59	—	[11,12]
24	0	405	412/434	470	474	11	—	
25	0	406	412/430	472	486	5	—	

Table 2. Cont.

Dye No.	Charge	$\lambda_{\text{abs}}^{\text{f}}$	$\lambda_{\text{abs}}^{\text{b}}$	$\lambda_{\text{fl}}^{\text{f}}$	$\lambda_{\text{fl}}^{\text{b}}$	$I_{\text{fl}}^{\text{b}}/I_{\text{fl}}^{\text{f}}$, $\varphi_{\text{fl}}^{\text{b}}$ (%)	K_{b} , τ^{DNA} , LOQ	Refs.
		nm						
40	+2	511	515	—	532	28%	LOQ = 70 ng/mL	
41	+2	502	508	—	527	18%	—	
42	+2	513	515	—	532	26%	—	[51]
43	+2	506	508	—	530	32%	—	
44	+1	508	516	—	529	27%	—	
45	+1	513	520	—	536	0.6	—	
52	+1	435	440	483	480	182	—	
53	+1	446	450	483	483	202	—	
54	+1	440	440	485	485	218	—	[60]
55	+1	442	442	485	488	166	—	
56	+1	441	445	479	483	177	—	
57	+1	442	447	485	483	198	—	
58	+1	400	400	433	426	55	—	
59	+1	422	425	471	462	85	—	
60	+1	413	413	465	460	34	—	[63]
61	+1	437	425	520	495	70	—	
62	+1	446	447	475	485	95	—	
63	+1	461	465	515	520	96	—	
64	+1	456	461	511	514	61.4	—	[63]
65	+1	488	495	640	575	150	—	
66	+1		440		487	19.14	$K_{\text{b}} = 1.01 \times 10^4 \text{ M}^{-1}$	[64]
67	+1	475	—	630	499	360	—	
68	+1	452	—	545	481	50	—	
69	+1	474	—	495	499	20	—	
70	+1	453	—	518	480	40	—	[65,66]
71	+1	474	—	599	498	250	—	
73	+1	476	—	500	499	100	—	
75	+1	461	—	512	515	5	—	
76	+1	494	498	530	525	1500, 69%	$\tau^{\text{DNA}} = 6.94 \text{ ns}$	[73,81]
77	+1	498	480	528	520	1000, 64%	$\tau^{\text{DNA}} = 6.84 \text{ ns}$, $K_{\text{b}} = 4.3 \times 10^6 \text{ M}^{-1}$	[81]
79	+2	486	494	550	543	1000, 66%	$\tau^{\text{DNA}} = 8.58 \text{ ns}$	[74,81]
80	+1	491	511	—	—	18%	$K_{\text{b}} = 1.4 \times 10^6 \text{ M}^{-1}$	
81	+1	464	492	—	—	100%	$K_{\text{b}} = 8.5 \times 10^6 \text{ M}^{-1}$	
82	+1	487	503	—	—	76%	$K_{\text{b}} = 4.6 \times 10^6 \text{ M}^{-1}$	[75]
88	+1	488	515	—	—	68%	$K_{\text{b}} = 5.8 \times 10^6 \text{ M}^{-1}$	
89	+1	514	535	—	—	14%	$K_{\text{b}} = 2.3 \times 10^6 \text{ M}^{-1}$	
90	+2	448	467	542	492	16	—	
91	+2	482	463	588	487	340	—	[79]
92	+2	487	516	590	561	130	—	
93	+1	510	532	535	546	1600	$\tau^{\text{DNA}} = 0.62 \text{ ns}$	
94	+1	512	536	537	553	2500	$\tau^{\text{DNA}} = 0.86 \text{ ns}$	
95	+1	520	552	592	600	3900	$\tau^{\text{DNA}} = 1.5 \text{ ns}$	[80]
96	+1	524	561	605	612	1700	—	

4.2. Dimeric MCD Probes

Additionally, widely used as probes are dimeric MCDs based on TO, YO, benzothiazole orange, etc., in which pairs of cyanine chromophores are linked by cationic bridges (in particular, TOTO and YOYO; **98** and **99**, respectively; see Figure 25) [25,46,52–54,81–88]. The general scheme for the synthesis of dimeric MCDs having 4 positive charges is shown in Figure 8 (see the previous section).

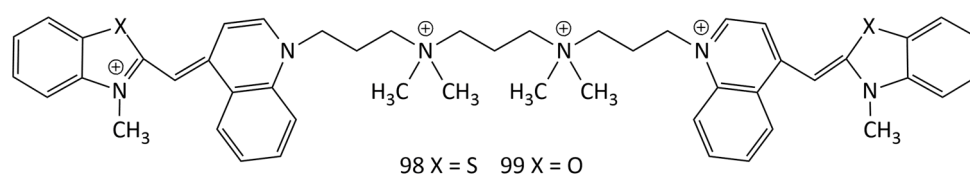


Figure 25. Structural formulas of dimeric MCDs **98** (TOTO) and **99** (YOYO).

The dimeric dyes **98** and **99** practically do not fluoresce in solution, but upon interaction with dsDNA form electrophoresis-resistant complexes with a greater than 1000-fold fluorescent growth [46]. The stability of complexes of dye **98** with ssDNA was studied in [82] by transferring TOTO from complexes to an excess of unlabeled DNA using gel electrophoresis. Complexes of **98** with DNA were also studied using spectral-fluorescent and CD spectroscopy. It was shown that the affinity of the polycationic dyes for ssDNA and dsDNA could be equally high. In [81], the interaction of dyes of various types (in particular, **99**, **76**, **77**, and **79** (see Figure 22) with ssDNA and dsDNA was studied. Upon the interaction with ssDNA, a broadening of the absorption and fluorescence bands was observed (compared to those of dsDNA). With gel electrophoresis, MCD **98** and **99** allow the determination of restriction fragments of nucleic acids from 600 to 24,000 base pairs. The limit of detection for dsDNA on agarose gel was 4 pg (excitation with a confocal laser), which is about 500 times better than that for ethidium bromide [46]. It was shown in [87] that homodimeric MCDs demonstrate strong fluorescent growth upon binding to ssDNA and dsDNA (LOD (dsDNA): ~1.7 ng/mL). An increase in the fluorescence intensity of **98** and **99** by three orders of magnitude upon binding to nucleic acids dyes was noted in [88]. The dependence of fluorescence intensity on the DNA concentration is linear in the range from 0.5 to 100 ng/mL (for dye **98** complexed with DNA; see PDB structure 108D [84]).

Binding of **98** and **99** to DNA and oligonucleotides was also studied by one and two-dimensional ^1H NMR spectroscopy [84–86]. Dyes **98** and **99** tend to form several types of complexes with dsDNA; the interaction with oligonucleotides occurs due to bisintercalation. In this case, the main factors in the stabilization of dye–DNA complexes are non-electrostatic forces (hydrophobic interactions and hydrogen bonds). In [89] the interaction of intercalating dyes **5** and **99** with dsDNA was studied using a combination of fluorescence optical microscopy and an optical tweezer setup. It has been shown that intercalation of the dyes between DNA base pairs leads to strand elongation. Total internal reflection fluorescence microscopy (TIRF) was used to elucidate the kinetic characteristics of MCD **99**'s interaction with DNA [90].

The interaction of dyes **5**, **99** and their derivatives with DNA was investigated using fluorescence stationary and ultrafast time-resolved techniques to elucidate the mechanism of MCD emission growth [91]. It was shown that the formation of H-dimers (weakly fluorescent) is less effective than the formation of MCD isomers for obtaining a good emission contrast. Optimization of the structure of molecules (in particular, the introduction of additional cationic groups) can reduce the contribution of aggregation and increase the sensitivity of probe dyes.

The interaction of four monomeric and dimeric MCDs, **14** (Figure 13), **5**, **48** (Figure 18), and **99** (Figure 25), with bacteriophage T5 was investigated in [45]. The studied MCDs were shown to penetrate inside the viral capsid and bind to the viral nucleic acid. The rate of binding also depends on the structure of the dye molecule; an increase in the size of the molecule slows down the process. At 37 °C, for monomeric MCD **14**, the process takes several minutes, while for dimeric **99** it takes more than 50 h.

The high sensitivity and stability of the complexes of dimeric MCDs with nucleic acids explain the research interest in new compounds of this type. The study of the interaction of dimeric MCD **100–103** (Figure 26) with ds-polynucleotides and poly-rA–poly-rU showed the selectivity of new dyes for GC base pairs compared to that of AT [27]. The presence of a positively charged linker results in a significant increase in the fluorescence intensity of the dyes upon binding to GC nucleotides (with AT, the increase is much lower). In experiments

on thermal melting, the dimeric dyes are characterized by weaker stabilization of DNA polynucleotides (weaker than that of the monomeric analogues), which is a consequence of the aggregation of **100–103** inside the hydrophobic grooves of polynucleotides (CD spectroscopy also showed aggregation).

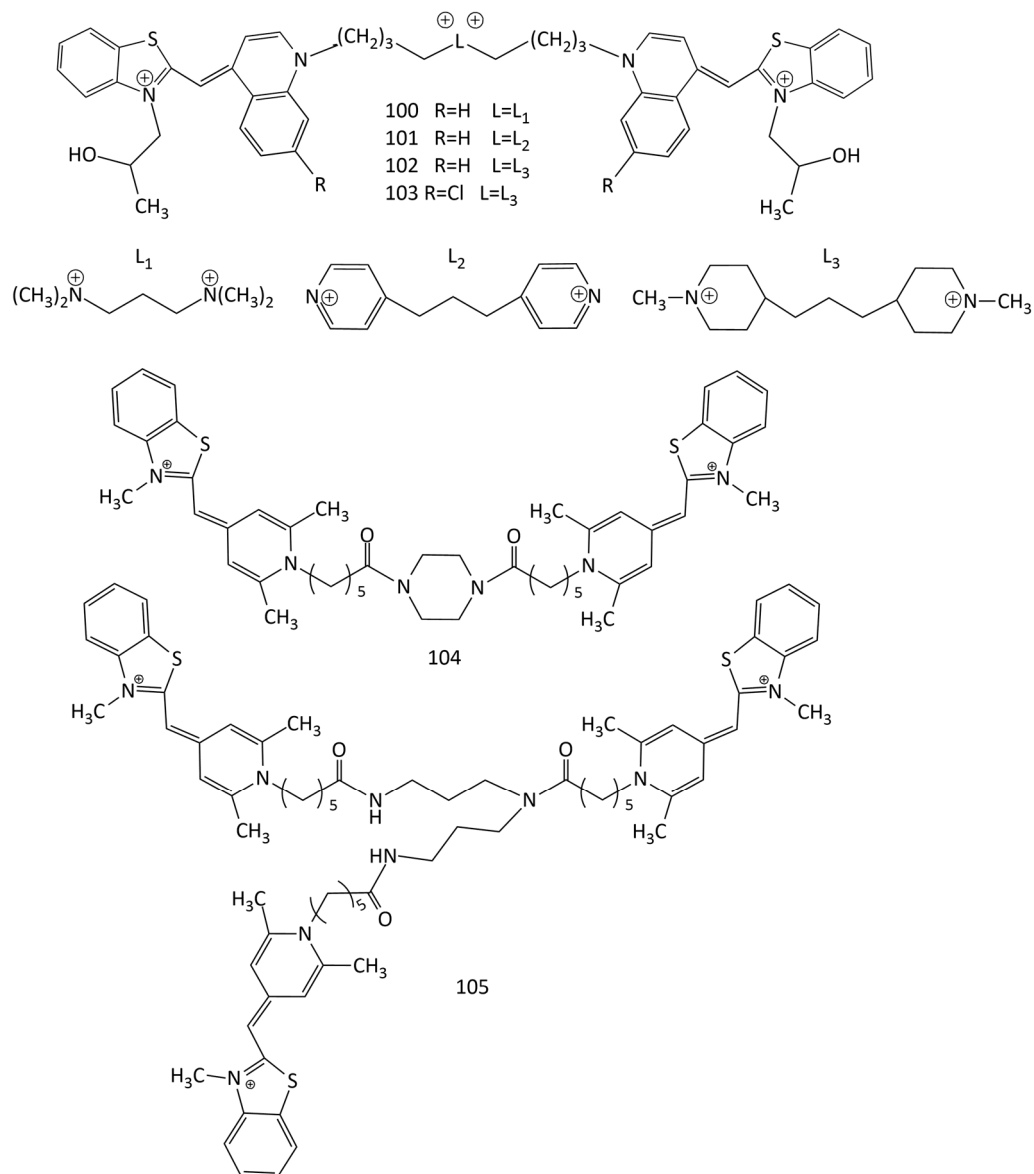


Figure 26. Structural formulas of homodimeric (**100–104**) and trimeric (**105**) MCDs with various linkers.

Dimeric and trimeric cyanine dyes **104** and **105** (Figure 26) based on pyridocyanine **52** (see Figure 19) were obtained [92]. The spectral-fluorescent properties of the synthesized dyes and their complexes with nucleic acids were studied. In the absence of DNA, the dyes are mainly in the form of H-aggregates; interaction with DNA leads to their decomposition and the formation of highly fluorescent complexes of monomeric dyes. Under conditions of excess DNA, the trimeric dye **105** shows a 1.5–3-times higher increase in the fluorescence intensity than the dimeric dye **104** does. With an excess of the dyes, the formation of H-aggregates on DNA is observed (DNA-induced aggregation). These aggregates have different spectral properties than the dye aggregates without DNA do. This effect can be used for more sensitive detection of DNA [92].

The data on the spectral-fluorescent studies of the interaction of homodimeric MCDs with DNA are summarized in Table 3.

Table 3. Spectral-fluorescent properties of homodimeric MCD probes in the absence (f) and in the presence (b) of dsDNA. λ_{abs} and λ_{fl} are maxima of the absorption and fluorescence spectra, respectively; I_{fl}^{f} and I_{fl}^{b} are fluorescence intensities in the absence and in the presence of dsDNA, respectively, $I_{\text{fl}} = I_{\text{fl}}^{\text{b}} - I_{\text{fl}}^{\text{f}}$; K_{b} is the constant of dye binding to DNA; τ^{DNA} is the fluorescence lifetime in the presence of DNA; and LOD is the limit of DNA detection.

Dye No.	Charge	$\lambda_{\text{abs}}^{\text{f}}$	$\lambda_{\text{abs}}^{\text{b}}$	$\lambda_{\text{fl}}^{\text{f}}$	$\lambda_{\text{fl}}^{\text{b}}$	$I_{\text{fl}}^{\text{b}}/I_{\text{fl}}^{\text{f}}$, I_{fl} (a.u.)	K_{b} , τ^{DNA} , LOD	Ref.
		nm						
98	+4	481	513	—	533	1400	$\tau^{\text{DNA}} = 1.96$ ns, LOD ~ 4 pg/mL (gel)	[42,46,82]
99	+4	488	489	549	509	3200	$K_{\text{b}} = 3.9 \times 10^6 \text{ M}^{-1}$, $\tau^{\text{DNA}} = 2.3$ ns, LOD ~ 1.7 ng/mL (sol.)	[42,81,82,87–89]
100	+4	478, 509	488, 525	—	548	157 a.u.	$K_{\text{b}} = 9.8 \times 10^5 \text{ M}^{-1}$	[27]
101	+4	484, 511	494, 525	—	538	386 a.u.	$K_{\text{b}} = 2.3 \times 10^6 \text{ M}^{-1}$	
102	+4	478, 521	490, 525	—	550	340 a.u.	$K_{\text{b}} = 4.5 \times 10^6 \text{ M}^{-1}$	
103	+4	486, 523	490, 525	—	538	216 a.u.	$K_{\text{b}} = 1.05 \times 10^6 \text{ M}^{-1}$	
104	+2	452	—	482	482	775	—	[92]
105	+3	452	—	482	482	1542	—	

4.3. Aggregation of MCDs on Nucleic Acids

Aggregation of MCDs on nucleic acids often accompanies the interaction of the monomeric dyes with the biopolymers [27,41,59] (see above). In particular, symmetrical MCD 2 forms J-aggregates on DNA, which were studied via LD and CD [41,93]. The recent work [94] reports the formation by dye 2 on ssDNA and dsDNA oligonucleotides of a new type of supramolecular aggregate, the photonics of which differ from those of H- and J-aggregates. Aggregation of dye 2 was studied using CD spectroscopy and atomic force microscopy. These superaggregates have the ability to effectively delocalize electronic excited states via the mechanism of exciton migration. It has been shown that the properties of the aggregates can be controlled by modifying the DNA substrate. Electronic excitation energy transfer (FRET) from dye 2 aggregates (donors) to AlexaFluor™ 647 (acceptor) was found and studied [94].

DNA-induced aggregation is also characteristic of unsymmetrical MCDs [27,95]. In particular, dyes 1 and 61 [95] form aggregates on DNA that are characterized by an abnormally large Stokes shift. In the unbound form, the dyes form H-aggregates in solution; in the presence of dsDNA with a 3–5-fold excess of the dyes, aggregates are formed from the free dye and DNA-bound dye (within the “half-intercalation” model). It has been found that benzothiazole MCD 106 (Figure 27) forms ordered dye aggregates on dsDNA templates. It has been shown that these aggregates can serve as efficient energy transfer “wires” in the process of electronic excitation energy transfer from donor to acceptor dye molecules with very small energy loss [96].

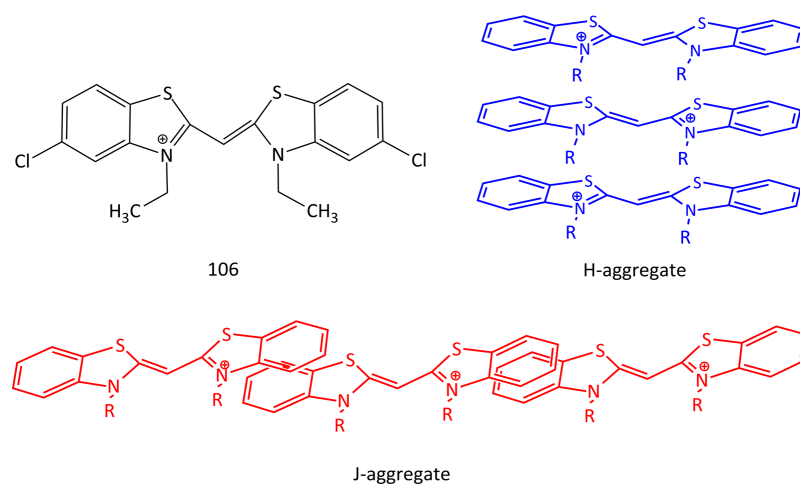


Figure 27. Structural formula of MCD 106 and possible structures of H- and J-aggregates of cyanine dyes.

Homodimeric and homotrimeric MCD **104** and **105** (Figure 26) form H-aggregates on DNA with an excess of the dyes with respect to the biopolymer, which increases the sensitivity of DNA detection [92,95,97]. Aggregation of dimeric MCD **100–103** in the presence of DNA is reported in [27]. The schematic structures of H- and J-aggregates of cyanines are shown in Figure 27.

4.4. MCD Probes for Non-Canonical Forms of DNA (G-Quadruplexes, Left-Handed DNA, etc.)

At present, investigations of MCD with polynucleotides of different structures continue, and efforts are being made to identify specialized fluorescent reporters for particular polynucleotides and non-canonical forms of DNA. Structures of canonical and some non-canonical forms of DNA are shown in Figure 28.

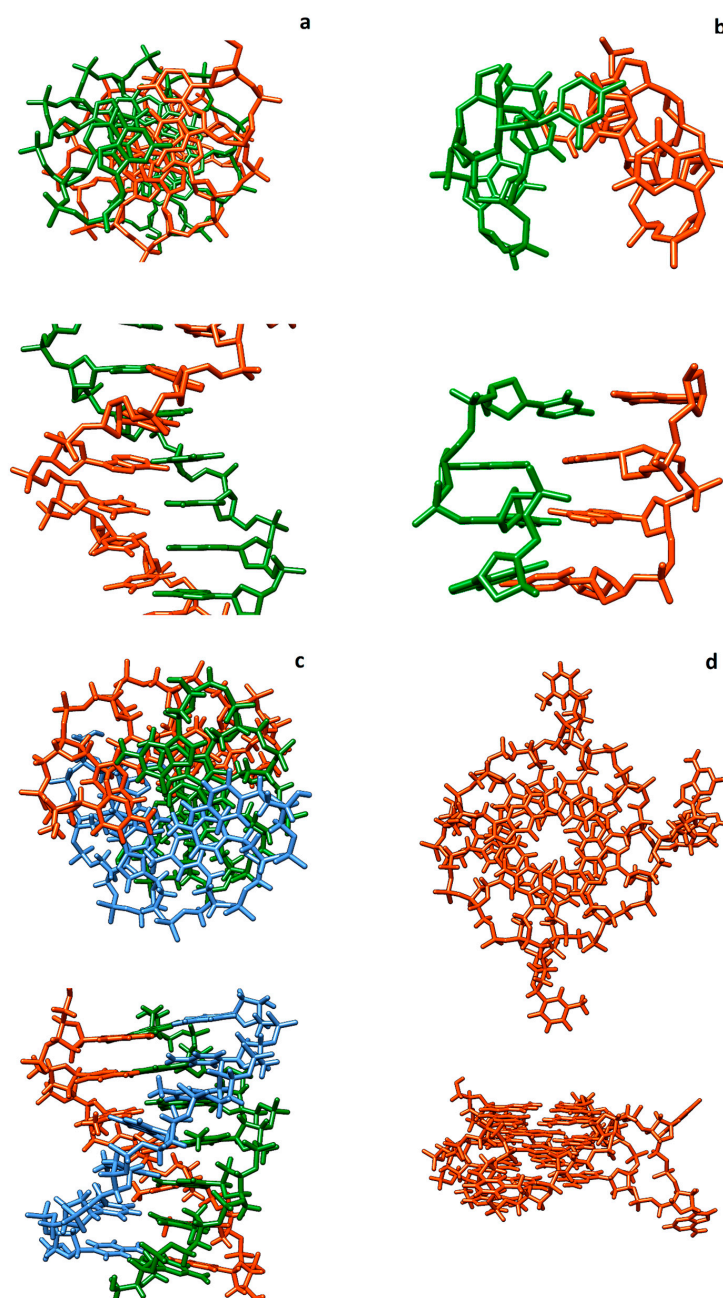


Figure 28. Structures of canonical and some non-canonical forms of DNA: canonical double helix ds-DNA structure ((a); B-DNA), left-handed DNA helix ((b), Z*-DNA), DNA triple helix (c), and DNA G-quadruplex (d).

The interaction of dye **1** with left-handed DNA (Z^* -DNA) was studied in [98]. Z^* -DNA is formed from B-DNA under the action of alcohol additions or doubly charged Mg^{2+} ions. Dye **1** interacts with Z^* -DNA via a two-step sequential mechanism. At the first stage, electrostatic interactions predominate; at the second stage, the dye is deeply embedded in the biopolymer. The specificity of the interaction between **1** and Z^* -DNA was discussed. In [13], the interaction of MCD **82–86** (Figure 23) with various types of nucleic acids was studied. The dyes showed a significant increase in fluorescence intensity. In [94], aggregation of **2** upon the interaction with DNA DX-tile nanostructures was studied.

DNA G-quadruplexes (G4) are guanine-enriched oligonucleotides or polynucleotides capable of forming four-stranded structures in the presence of singly charged cations (K^+ ions). In this case, four guanidine residues form a planar structure stabilized by guanine (G)-quartets (eight hydrogen bonds in total). It is known that G4 are located in DNA at the ends of eukaryotic chromosomes (telomeres). The function of telomeres is to protect chromosome ends from unwanted damage resulting from recombination or the action of nucleases.

It has been shown [43] that dye **1** binds more effectively to double-stranded (ds) DNA (with the formation of intercalation complexes) than to single-stranded oligonucleotides. Dye **1** also interacts with triplexes and G-quadruplexes of DNA [99,100]. Binding of dye **1** with three-stranded or four-stranded DNA structures leads to an increase in the dye fluorescence intensity by more than 1000 times. Complexes of **1** with triplexes and G-quadruplexes of DNA exhibit high stability and do not dissociate during chromatography and gel electrophoresis procedures [100].

The interaction of **52** with triplexes and G-quadruplexes of DNA was studied [101]. Dye **52** was shown to form very stable, highly fluorescent complexes with a DNA triple helix. The intercalation model describes the complexation of MCD with a DNA G-quadruplex, whereas binding of the dyes to triplexes is probably carried out in the DNA groove.

It has been shown that benzoselenazolyl MCDs with a methyl substituent at the N-atom (dyes **20** and **21**; Figure 14) selectively detect DNA G-structures [12]. MCD **23** with a $(CH_2)_2SH$ group demonstrates differences in the CD spectra upon complexation with dsDNA, RNA, and G-quadruplexes. The results of the study show that the dyes bind to the G-quadruplex via terminal π - π stacking [12]. The possibility of additional stabilization of the complex due to non-covalent interactions with nucleic acid bases/phosphate backbone was shown.

4.5. MCD Probes for RNA

At present, a significant number of MCDs exhibiting selectivity for dsDNA have been developed and studied (many of them are considered above). However, relatively few probes are currently known that are suitable for the selective detection of RNA structures. In particular, bis-benzimide dye probes of the Hoechst type can be used to quantify RNA from the total nucleic acid content. However, the protocol requires the use of ribonuclease, which can reduce sensitivity and increase error [102]. A commercial fluorescent probe, SYTO RNaselect (www.thermofisher.com; accessed on 4 May 2023), with high RNA specificity is also available [103].

The works [104,105] proposed new unsymmetrical MCDs with benzo[c,d]indole and quinoline nuclei as fluorescent probes for RNA (dyes **107–109**; Figure 29). The presence of the benzo[c,d]indole residue significantly shifts the maxima of the absorption and fluorescence spectra of the dyes to longer wavelengths. The presence of side substituents with amino groups improves the interaction with RNA; the RNA selectivity and stability of these dyes is higher than that of SYTO RNaselect. When interacting with RNA, the fluorescence intensity of the dyes in the deep-red spectral region (~657–666 nm) increases by more than 100 times. The fluorescent response of the dyes with aminopropyl groups (**108** and **109**) for RNA was 2.2–3.4 times higher than that of the methyl-substituted dye, **107**; it was also much higher than that for dsDNA. The association constants were of the order of $1.25\text{--}4.8 \times 10^3 \text{ M}^{-1}$.

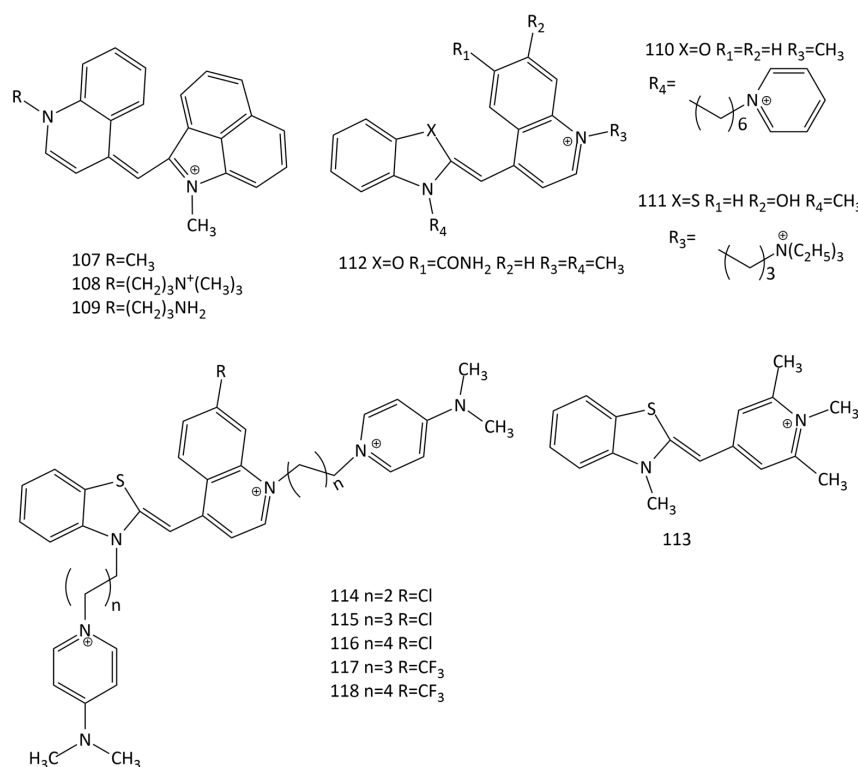


Figure 29. Structural formulas of unsymmetrical monocationic and dicationic MCDs **107–118**.

The interaction with DNA and RNA of five unsymmetrical monocationic and dicationic MCD (dyes **64** and **110–113**; Figure 29) was studied in [106]. Upon the interaction with yeast total RNA, a 1.3–5.3-fold greater increase in the fluorescent response was observed than that observed in the presence of dsDNA (with a maximum selectivity increase of 5.3 times for dye **113**).

The synthesis and interaction with DNA and RNA of new MCDs **114–118** (Figure 29) were described [107]. The electronic spectra were analyzed using TDDFT. The dyes practically do not fluoresce in the unbound state. When interacting with nucleic acids, the spectra of the dyes are shifted to the long-wavelength side by 2–6 nm, and an increase in the fluorescence intensity of the ligands is observed (for dye **114** the increase in the presence of RNA is 114 times). When binding to RNA, the dyes with a Cl substituent (**114–116**) show a higher increase in the fluorescent response (for **114**, this is ~3 times higher) than with DNA. The CD spectra of the dyes showed optical activity—negative signals for dyes **114** and **117** in complexes with RNA—characteristic of intercalative binding [107].

The data from the spectral-fluorescent studies of the interaction of MCDs with RNA are summarized in Table 4.

Table 4. Spectral-fluorescent properties of MCD probes in the absence (f) and in the presence (b) of RNA. λ_{abs} and λ_{fl} are maxima of the absorption and fluorescence spectra, respectively; I_{fl}^{f} and I_{fl}^{b} are fluorescence intensities in the absence and in the presence of RNA, respectively; $\varphi_{\text{fl}}^{\text{b}}$ is the fluorescence quantum yield of the dye bound to RNA; and K_{b} is the constant of dye binding to RNA.

Dye No.	Charge	$\lambda_{\text{abs}}^{\text{f}}$	$\lambda_{\text{abs}}^{\text{b}}$	$\lambda_{\text{fl}}^{\text{f}}$	$\lambda_{\text{fl}}^{\text{b}}$	$I_{\text{fl}}^{\text{b}}/I_{\text{fl}}^{\text{f}}, K_{\text{b}}, \varphi_{\text{fl}}^{\text{b}}$ (%)	Refs.
		nm					
40	+2	511	—	—	646	—	[51]
41	+2	502	—	—	633	—	
42	+2	513	—	—	652	—	
43	+2	506	—	—	596	—	
44	+1	508	—	—	534	—	
45	+1	513	—	—	570	—	

Table 4. Cont.

Dye No.	Charge	$\lambda_{\text{abs}}^{\text{f}}$	$\lambda_{\text{abs}}^{\text{b}}$	$\lambda_{\text{fl}}^{\text{f}}$	$\lambda_{\text{fl}}^{\text{b}}$	$I_{\text{fl}}^{\text{b}}/I_{\text{fl}}^{\text{f}}, K_{\text{b}}, \varphi_{\text{fl}}^{\text{b}} (\%)$	Refs.
		nm					
52	+1	435	440	482	482	255	
53	+1	446	449	483	485	145	
54	+1	440	440	485	488	155	
55	+1	442	439	485	485	134	[60]
56	+1	441	445	479	483	130	
57	+1	442	447	485	483	143	
64	+1	462	468	524	506	180	[106]
75	+1	461	—	512	495	—	[66]
107	+1	580	624	—	645	$105, K_{\text{b}} = 1.25 \times 10^6 \text{ M}^{-1}$	[104,105]
108	+2	600	—	—	666	$350, K_{\text{b}} = 2.8 \times 10^3 \text{ M}^{-1}$	
109	+1	595	—	—	665	$230, K_{\text{b}} = 4.8 \times 10^3 \text{ M}^{-1}$	[105]
110	+2	480	489	515	511	306	
111	+2	465	506	608	529	402	
112	+1	468	504	564	526	479	[106]
113	+1	434	451	469	476	128	
116	+3	514	518	549	547	75	
117	+3	522	524	575	547	8	[107]
118	+3	520	523	558	554	70	

5. Interaction of MCD with Proteins and Other Biomolecules

A number of new MCDs as possible fluorescent probes for proteins have been synthesized and studied [108]. The dyes were synthesized on the basis of the “affinity-modifying groups” idea, using MCD 52 (Figure 19) as a model. It was shown that specific and accurate detection of bovine serum albumin is possible using dyes 119, 120 and 121 (Figure 30). In particular, for 119 and 120, a ~100-fold fluorescence growth is observed in the presence of albumin.

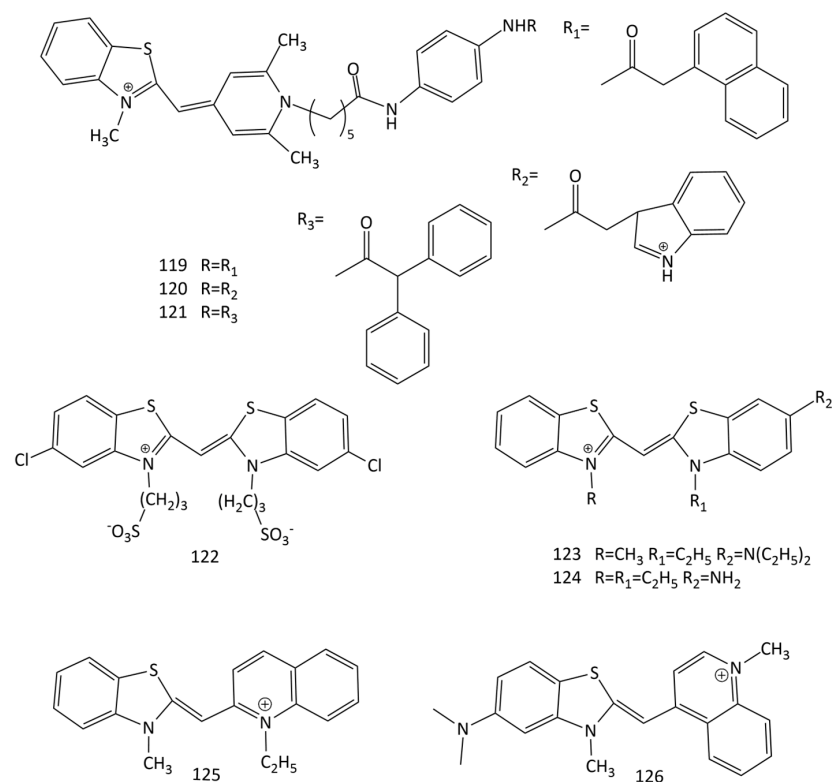


Figure 30. Structural formulas of MCDs 119–126.

The interaction of the symmetrical anionic MCD **122** (Figure 30), having two sulfo-propyl substituents in 3,3' positions, with two artificially synthesized polypeptides was studied in [109]. Using UV-Vis, CD spectroscopies, and Cryo-TEM microscopy, it was that, depending on the concentration in the aqueous medium, the dye is in the form of H- or J-aggregates; polypeptide molecules, in turn, form α -helical supramolecular ensembles and β -sheet-rich fibrils. The interaction of **122** with polypeptides leads to the formation of new supramolecular structures of tubular aggregates [109]. CD spectra showed no chirality transfer from peptides to the dye aggregates, and also permitted excluding the opposite effect of a structural transfer from dye aggregates to the peptides' secondary structure.

J-aggregate formation by dye **122** in the presence of some proteins (gelatin, lysozyme, ribonuclease, and trypsin) was studied using CD [110]. It was shown that the chirality of proteins controls the optical activity of MCD J-aggregates.

Currently, a search is underway for fluorescent probes with specificity for amyloid protein structures; the relevance of these studies is associated with the therapy for a number of neurological disorders. In order to detect fibrillar β -lactoglobulin, two cationic MCDs based on benzothiazole heterocycles, **59** and **123** (Figure 30), were studied (along with a number of trimethine, pentamethine, heptamethine cyanine and squarylium dyes) [111]. The fluorescent response of these dyes for fibrillar β -lactoglobulin was ~ 3 times higher than that for native β -lactoglobulin.

Additionally, a search for MCDs that detect amyloid form of α -synuclein was performed (in particular, MCDs **1**, **52**, **59**, **62** and **123–126** (Figure 30) were studied) [112–114]. The best results were obtained for dye **123**, for which the fluorescence response for fibrillar α -synuclein was 9.5 times higher than that for native α -synuclein.

The interaction of a series of MCDs (dyes **127–131**; Figure 31) with insulin and lysozyme in the native and amyloid states was studied [115]. It was found that the emission of MCDs is enhanced by the binding of the dyes with both native and fibrillar proteins. In fibrillar protein–MCD complexes, the effect is stronger than in the cases of proteins in the native form. However, their amyloid (fibrillar) selectivity is much lower compared to that of other amyloid markers [115]. The maximum amyloid detection factors characterizing the selectivity of the dyes toward fibrillar insulin and lysozyme were found to be 8.4 for dye **128** and 5.5 for dye **130**. The dyes also show a relatively higher increase in the fluorescence intensity in the presence of insulin amyloid fibrils in comparison with that in the presence of lysozyme, suggesting the sensitivity of the dyes to the fibril morphology.

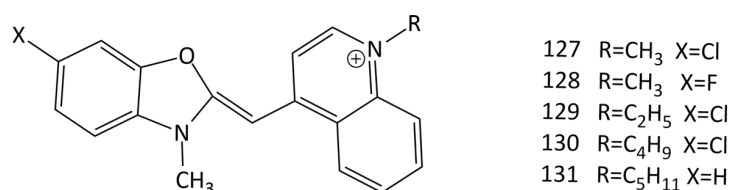


Figure 31. Structural formulas of MCDs **127–131**.

To identify the monomethine–protein binding sites, the molecular docking technique was used. Residues of the B-chain (Val 17, Leu 17, Ala 14, Phe 1, Gln 4, and Leu 6) and A-chain (Leu 13, Tyr 14, and Glu 17 of insulin) show the MCDs' binding efficiency and seem to form the strongest complexes with the dyes. It was found that the binding of the investigated cyanines is governed predominantly by hydrophobic interactions between the dye molecule and the insulin residues Val 17, Leu 17, Ala 14, Gln 4, Leu 6, Leu 13, Tyr 14, and Glu 17. Moreover, all the examined dyes tend to form π -stacking contacts between the benzene ring and Phe 1 residue of the B-chain of non-fibrillar insulin. According to molecular docking results, the fibrillar insulin Gln15_Glu17 groove is the most effective binding location for the MCDs under investigation [115].

The interaction of **127–131** (Figure 31) with bacteriophage MS2 was studied [116]. The dyes interact with the bacteriophage with high affinity ($\sim 1 \mu\text{M}^{-1}$); evidence was presented to support the hypothesis of dye interaction with viral nucleocapsid proteins. Molecular

docking showed the possibility of accommodating a dye molecule inside the cleft formed by three proteins composing the virus shell.

The work [117] reports the formation of J-aggregates of dye **2** on the surface of heparin (stimulated aggregation) with a ~400-fold increase in the fluorescence intensity. A strong bisignate signal appears in the CD spectra as a result of excitonic coupling between dye molecules in J-aggregates. Dye **2** exhibits selectivity for heparin; the fluorescence intensity in the presence of heparin is much higher than that in the presence of chondroitin sulfate and hyaluronic acid. The limit of detection of heparin is 2 nM.

6. Photonics of the Dye Molecules in Complexes with Biomolecules

Time-resolved ultrafast fluorescence spectroscopy (TRFS) was used to determine the fluorescence growth mechanism of dyes **5**, **14**, and **99**, as well as their derivatives, in the presence of nucleic acids [91,118]. It has been shown, in particular, that in complexes with DNA the fluorescence lifetimes of the dyes become much longer because of the constrictive DNA environment which inhibits torsional nonradiative deactivation of the dyes' excited state. Similar data were obtained for dye **5** and its derivatives using femtosecond fluorescence up-conversion spectroscopy [35].

One of the most important properties of cyanine dyes in association with biomacromolecules is their ability to inhibit the processes of nonradiative deactivation. As was shown for trimethine cyanines, this can lead to a significant increase in the quantum yield of the triplet state (Φ_T) [3]. The triplet state of the dye can produce reactive oxygen species (ROS). Since Φ_T is usually close to zero for cyanine dyes in the free state, it is generally possible to create highly selective agents for photodynamic therapy (PDT), in which only cyanine dye molecules bound to biomolecules will have a damaging effect, while unbound dye molecules will be inactive.

In the case of MCD, the effect of an increased Φ_T was observed for dye **99** (YOYO) in a complex with DNA. In [119], the interaction of dye **99** with DNA fragments of various lengths was studied using fluorescence correlation spectroscopy (FCS). An increase in Φ_T was found in the system, depending on the length of DNA molecules and the DNA/YOYO ratio. The results obtained are proposed to be used for the development of fluorescence cross-correlation spectroscopy techniques in solutions and in living cells.

A new MCD probe sensitive to DNA hybridization was obtained (**132**, Figure 32) [120]. A nucleic acid fragment and two TO fluorophores constitute the dye **132** molecule. Through hybridization with the target DNA, the population of the transient dark state, which is attributed to the triplet state and isomerized state, was drastically increased. According to FCS results, the transient dark state population (attributed to the triplet state and isomerized state) was found to significantly increase through hybridization with the target DNA.

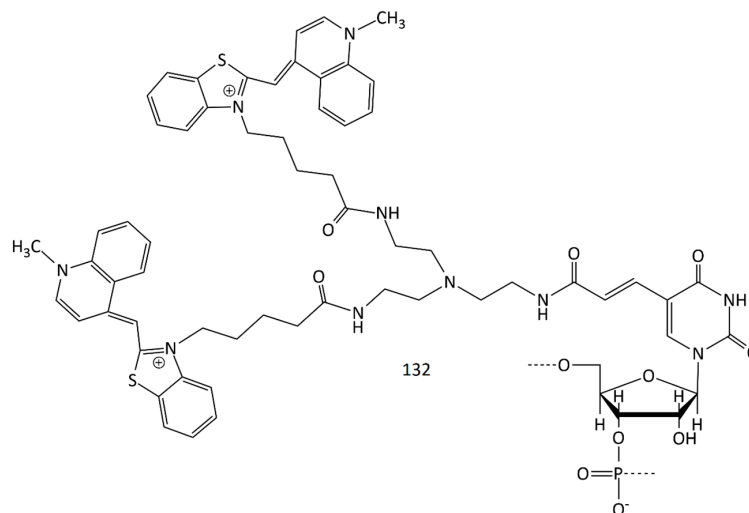


Figure 32. Structural formula of the dimeric dye **132**.

Thus, due to the set of their exceptional characteristics, the use of MCDs opens up broad prospects for the development of methods for biomolecule detection/analysis and for the design of new types of molecular probes.

7. Application of Monomethine Cyanine Dyes in Biochemistry and Biomedicine

The outstanding ability of MCDs to greatly enhance the fluorescent response in the presence of biomacromolecules determines the main areas of application of monomethine cyanines. The most important are fluorescent probes and stains for biomolecular analysis, off-on sensors and markers, and visualization of biomacromolecules in biological systems [121]. The application of MCDs as fluorescent probes was considered in detail in the preceding sections. More specific applications of MCDs are considered below.

MCDs of various types are often used in bioanalysis (FFC, PCR methods, fluorescent microscopy, etc.) Dyes **1** and **14** (see Figures 1 and 13) are widely used in modern biomedical practice; in particular, **1** is used in fluorescence-activated cell cytometry (in reticulocyte analysis, the use of dye **1** gives a higher correlation coefficient compared with manual determination) [5]. Flow cytometry also uses monomeric and dimeric MCDs; in particular, **98** (TOTO) and **47** (TO-PRO) [122], **99** (YOYO-1), **5** (YO-PRO-1), and **77** (PicoGreen) [123]. MCD **76** (SYBR Green I), **99** (YOYO-1), **98** (TOTO-1), and **77** (PicoGreen) are used in flow virometry—a new method for characterization of viruses [124]. The possibility of practical application of YO derivatives—dyes **127–131** (Figure 31), as noncovalent fluorescent markers of bacteriophage MS2 was shown in [116]. In the presence of MS2, the dyes showed a significant fluorescent growth, which made it possible to detect low virus concentrations (~2–20 nM/mL). The results outlined in [116] can be used to develop fluorescent viral markers.

For spectral-fluorescent detection of dsDNA in gel electrophoresis, for quantitative detection of dsDNA in solution, and real-time PCR, the commercially available dyes SYBR Green I, PicoGreen, SYBR Green II, and SYBR Gold (**76–79**; Figure 22) have been developed and widely used [67–71].

Unsymmetrical MCDs are proposed to be used in fluorescence microscopy for staining RNA-containing cell organelles. When staining live and fixed biopreparations of MCF-7 cells, dyes **64** (Figure 20) and **110–113** (Figure 29) penetrate well into cells and nuclei [106].

Unsymmetrical monomethine cyanines with benzo[*c,d*]indole and quinoline nuclei were proposed as selective fluorescent off-on probes for RNA (quantitative detection of RNA in vitro and visualization of nucleolar RNA in vivo) (dyes **107–109**; Figure 29) [104,105]. Dye **133** (Figure 33), proposed in [125], exhibited significant advantages over SYTO RNA select. In particular, dye **133** is characterized by a stronger fluorescent response than SYTO RNA select is upon binding to RNA in the cell nucleoli. Dye **133** exhibited good results in terms of cytotoxicity and permeability through cell membranes.

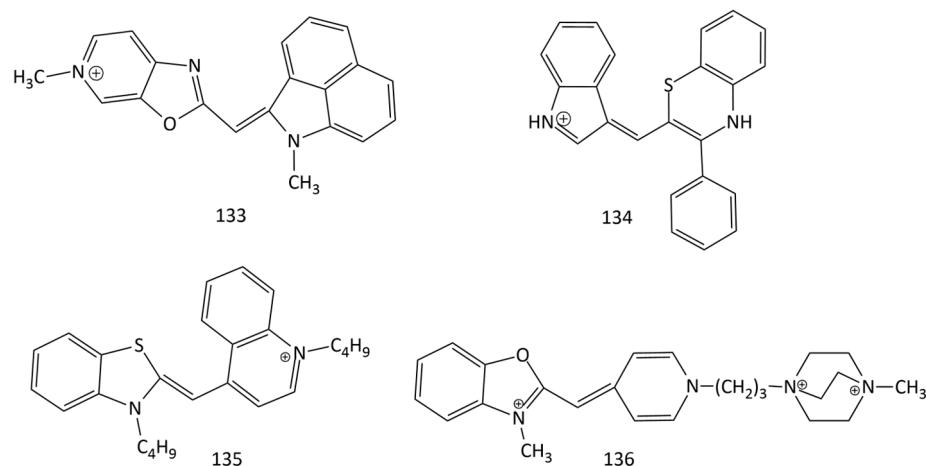


Figure 33. Structural formulas of dyes 133–136.

J-aggregation of dye **2** (PIC) was considered for the detection of heparin in serum samples and complex biological media [117].

Based on benzothiazine, new MCD, **134** (Figures 6 and 33), with reversible acidochromic behavior was obtained. Sensitivity to pH changes makes this dye an attractive prototype of a new modular chromophore [22].

In [126], MCDs **135** (Figure 33) and **98** (Figure 25), together with various dimethine and trimethine cyanine dyes, were studied for dsDNA (lambda phage DNA) quantification using gel electrophoresis. MCD **135** (a butyl homologue of **1**) can be proposed for DNA detection; this dye proved to be more sensitive than the commonly used ethidium bromide did. Of all dyes studied, the most sensitive were **98** and **135**.

A high-sensitivity method for DNA detection with MCDs using the stopped-flow technique was proposed. It was based on measuring the initial rate of dye **99** (YOYO)'s fluorescent growth in the presence of sodium dodecyl sulfate upon the introduction of DNA. This method makes it possible to detect very low concentrations of DNA ($\sim 3.0 \times 10^{-10}$ M) [127].

Monomethine N-aryl pyridocyanines (dyes **93–97**; Figure 24) [80] are proposed as new types of cell markers for fluorescence spectroscopy. In mammalian cells and plant cell preparations, dyes **93–97** stain both nuclear and organelle DNA. The dyes are suitable for imaging beyond optical resolution and in two-photon microscopy techniques; they can be used for deep-tissue imaging.

A new polycationic unsymmetrical MCD, **136** (Figure 33), was used to count the number and determine the viability of yeast cells using an image-based cytometry method [128]. The dye penetrates only into dead cells, binds rapidly to DNA (20 times faster than **99** does), and has a weak background and high sensitivity to DNA (in the presence of DNA, the dye has a fluorescence intensity that is 10 times higher than that of propidium iodide). The method proposed by the authors has a low coefficient of variation.

The results of studies of MCDs based on SYBR green II (dyes **82–86**; Figure 23) covalently bound to the viral capsid can pave the way for a further application of these compounds in biological objects for the detection of RNA in viruses [13].

To detect DNA mutations, sequence-specific forced intercalation hybridization probes based on dyes **1** and **14** were suggested [129–133]. Upon hybridization with corresponding target DNA, the fluorescence of the probes increased and was sensitive to structural disturbances of NA caused by the mismatch of neighboring bases. Dyes **137–140** were also tested [134]. Dyes **137–140** exhibit high affinity and can be used to detect matched and non-matched targets under non-stringent hybridization conditions.

In particular, single-molecule fluorescence spectroscopy (MFS) makes extensive use of MCD [135–137]. In [138], 12 monodimeric and homodimeric MCDs (in particular, dyes **141–145**, Figure 34) were studied using the single-DNA molecule technique in comparison with commercially available homodimeric MCDs (dye **99**, Figure 25). Monomeric dyes **141–144** and the dimeric symmetrical MCD **145** are quite photostable and were selected as prospective dyes for nucleic acid detection.

In living cells, monomethine cyanines are able to demonstrate not only an increase in fluorescence intensity, but also effects of inhibition of cell activity (that is, they have a theranostic potential). The work [12] provides data on the activity of selenocyanines **20–26** (Figure 14) against human cancer cells. Confocal microscopy data confirm the potential of the novel unsymmetrical MCDs **20–26** as theranostic agents. The dyes with sulfopropyl and thioethyl substituents accumulate in mitochondria, while cyanine with a methyl substituent is localized in the nucleus.

New MCDs (dyes **100–103**; Figure 26) were proposed as theranostic agents; the dyes showed cell growth-inhibitory effects on cancer cells (lines HCT 116; MCF-7 and H460) [21]. Screening against human lung carcinoma (A549) showed that guanidiniocarbonylpyrrole conjugates of MCDs accumulate effectively in cell mitochondria, causing moderate cytotoxic effects, which make them favorable for use in theranostics [49].

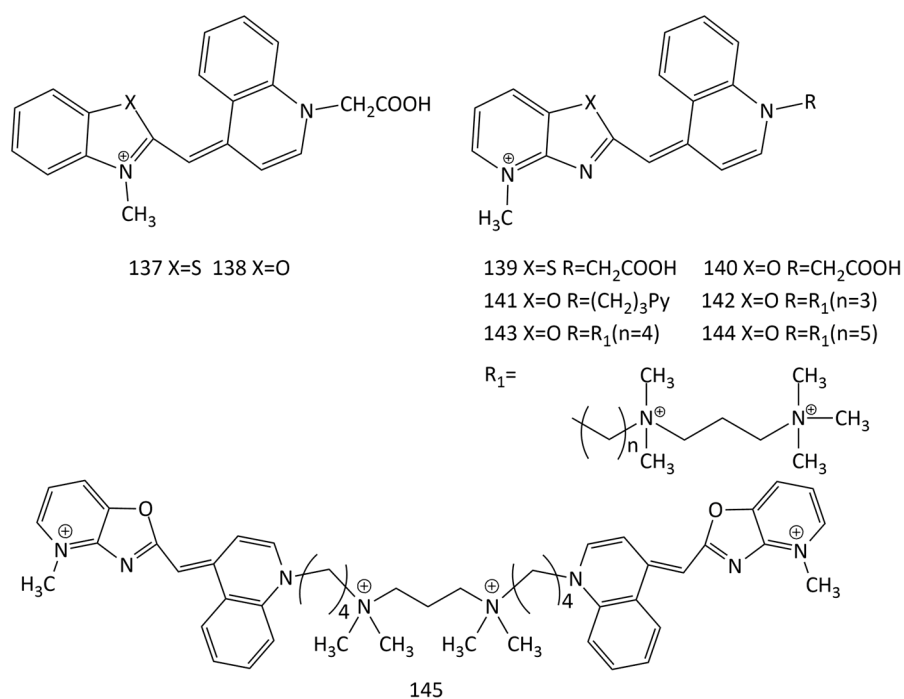


Figure 34. Structural formulas of dyes 137–145.

With encouraging success, photodynamic therapy (PDT), a non-invasive and general treatment strategy, is being used to treat pathogenesis (especially in the case of antibiotic resistance). Photosensitizers activated by light can generate excess amounts of reactive oxygen species (ROS) that can highly suppress or kill pathogens. Usually, cyanine dyes with a longer polymethine chain than that of MCDs are used in PDT [139]. Nevertheless, there are some studies on PDT with MCDs. The recent work [140] studied the photodynamic activity of the symmetrical “simplest” MCD, dye 146 (Figure 35), in a carbomer gel (CBMG) filler. As a part of the Cy-CBMG system, the solubility of the dye in water is significantly better, and photodegradation occurs less. Dye 146 in CBMG has good biocompatibility, effectively destroys antibiotic-resistant bacteria *in vitro*, and promotes wound healing *in vivo*.

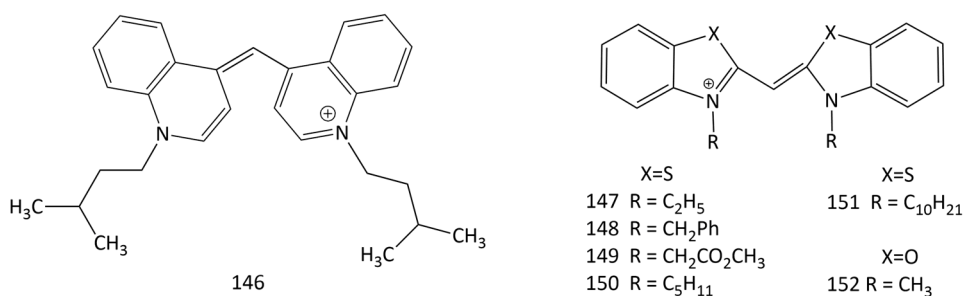


Figure 35. Structural formulas of dyes 146–152.

In the work [26], a number of dicationic analogues of **1** and tetracationic analogues of the dimeric dye **98** were synthesized. It was concluded that the dyes obtained indicate significance in singlet oxygen sensitization and are potential candidates in the area of PDT. For chalcogenopyrylium monomethine dyes (dyes **9–12**; Figure 11), an increase in Φ_T in viscous solvents and with Te-substitution was observed, which could be potentially used in PDT [34].

Cyanine dyes are actively studied as sensitizers in PDT, but their antiproliferative activity in the absence of light has been studied less. New work [8] is devoted to the study of the antiproliferative effects, selectivity, and the effect of light on the cytotoxic activity of

a number of cyanines (including symmetrical MCDs, that are butyl homologues of **3**; dyes **59** and **147–152**) in relation to human tumor cells. It is demonstrated that **147–152** have antiproliferative impacts on the Caco-2, MCF-7, and PC-3 cancer lines.

8. Conclusions

To date, a huge variety of MCD have been produced and investigated for nucleic acid detection and analyses. In addition, noncovalent interactions of various types of MCD not only with natural DNA and RNA, but also with a number of other polynucleotides and oligonucleotides and non-canonical forms of DNA were studied by spectral-fluorescent and other methods. Note that strong spectral shifts upon binding to nucleic acids are not typical of MCD probes (if this is not accompanied by decomposition and/or a formation of dye aggregates), but, as a rule, a significant upturn in fluorescence response is observed. A variety of MCDs were chosen as sensitive molecular reporters suited for the quantification of DNA in biological systems and for their use in various biophysical and biomedical applications. For example, the limit of dsDNA detection using TOTO and YOYO was found to be about 0.5 ng/mL, or 20 pg in a 25 μ L well [88]; dyes SYBR Green I and PicoGreen (**76** and **77**, respectively) can quantify dsDNA at concentrations of \sim 0.5–1 ng/mL [73].

Some MCD probes are commercially available from the following main suppliers: Merck (Sigma-Aldrich), Thermo Fisher Scientific, and Biosynth. Merck purchases TO (**1**), YO (**14**), SYBR Green I and II (**76** and **78**, respectively); Thermo Fisher Scientific purchases the TOTO (**98**) and TO-Pro (**47**) families of dyes, as well as SYBR Green I and II, PicoGreen (**77**), and SYBR Gold (**79**); Biosynth purchases TO, YO and SYBR Green I.

At the same time, it should be noted that a lot of MCD probes exhibit high sensitivity to DNA, but much less probes are highly sensitive to RNA, especially in the presence of DNA, showing high selectivity for RNA. Therefore, works devoted to the elaboration of sensitive cyanine dye probes selective for RNA against the presence of DNA are particularly valuable and require further development. Additionally, welcomed are studies on MCD probes for non-canonical forms of DNA: triplexes and G-quadruplexes, left-handed DNA, plasmid DNA, ssDNA, etc.

There are some common structure–activity relationships for dye probes that were revealed in studies of the dye–DNA interaction. The planar shape and compact size of MCD molecules are structurally better suited for the formation of DNA intercalation complexes. Larger, crescent-shaped MCD molecules often bind in the groove of DNA. (Poly)cationic substituents in dye molecules can substantially increase the affinity of MCDs to nucleic acids. Furthermore, several affinity-modifying groups in MCD molecules can drastically change the characteristics of the dye–nucleic acid interaction. These auxiliary groups have the ability to non-covalently bind to biopolymers and increase MCD affinity. Importantly, the presence of affinity-modifying groups in the MCD structure should not create addition steric barriers to MCD intercalation or nucleic acid groove binding [60].

In addition, in contrast to the great number of works on MCD probes for nucleic acids, a relatively small number of works on such probes for other biomacromolecules are available. This research area should also be developed. The creation of spectral-fluorescent probes for amyloid proteins is necessary because of the association of the latter with a wide range of neuropathies (for example, ALS, Parkinson's and Alzheimer's diseases, motor neuron diseases).

Finally, there are very few works on the study of photochemical processes in MCD molecules in complexes with biomacromolecules, primarily concerning the generation of the triplet state of a MCD and its quenching by molecular oxygen (and other triplet quenchers). In addition to fundamental significance, this study can give information about the peculiarities of localization of the ligand molecule in the biomolecular framework and its possible shielding from the access of a quencher molecule. This is also of great practical importance for PDT, since it creates the basis for the development of selective PDT agents. Such agents would be photochemically active (and could generate singlet oxygen) only in a complex with a target biomolecule and would be inactive in the free state.

Author Contributions: Conceptualization, A.S.T.; resources, A.S.T. and P.G.P.; writing—original draft preparation, A.S.T. and P.G.P.; writing—review and editing, A.S.T. and P.G.P.; funding acquisition, A.S.T. All authors have read and agreed to the published version of the manuscript.

Funding: This work was carried out under the State Assignment of IBCP RAS (state registry no. 001201253314).

Institutional Review Board Statement: Not applicable.

Informed Consent Statement: Not applicable.

Data Availability Statement: Data sharing is not applicable to this article.

Conflicts of Interest: The authors declare that they have no conflict of interest.

References

1. Mishra, A.; Behera, R.K.; Behera, P.K.; Mishra, B.K.; Behera, G.B. Cyanines during the 1990s: A review. *Chem. Rev.* **2000**, *100*, 1973–2011. [[CrossRef](#)] [[PubMed](#)]
2. Tatikolov, A.S. Polymethine dyes as spectral-fluorescent probes for biomacromolecules. *J. Photochem. Photobiol. C* **2012**, *13*, 55–90. [[CrossRef](#)]
3. Pronkin, P.G.; Tatikolov, A.S. Photonics of trimethine cyanine dyes as probes for biomolecules. *Molecules* **2022**, *27*, 6367. [[CrossRef](#)] [[PubMed](#)]
4. Williams, C.G. XXVI.—Researches on chinoline and its homologues. *Trans. Roy. Soc. Edinburgh* **1857**, *21*, 377–401. [[CrossRef](#)]
5. Lee, L.G.; Chen, C.H.; Chiu, L.A. Thiazole orange: A new dye for reticulocyte analysis. *Cytometry* **1986**, *7*, 508–517. [[CrossRef](#)]
6. Hamer, F.M. *The Cyanine Dyes and Related Compounds*; John Wiley & Sons: Hoboken, NJ, USA, 1964; p. 790.
7. Brooker, L.G.S.; Keyes, G.H.; Williams, W.W. Color and constitution. V. The absorption of unsymmetrical cyanines. Resonance as a basis for a classification of dyes. *J. Am. Chem. Soc.* **1942**, *64*, 199–210. [[CrossRef](#)]
8. Serrano, J.L.; Maia, A.; Santos, A.O.; Lima, E.; Reis, L.V.; Nunes, M.J.; Boto, R.E.F.; Silvestre, S.; Almeida, P. An insight into symmetrical cyanine dyes as promising selective antiproliferative agents in Caco-2 colorectal cancer cells. *Molecules* **2022**, *27*, 5779. [[CrossRef](#)]
9. Kaloyanova, S.; Trusova, V.M.; Gorbenko, G.P.; Deligeorgiev, T. Synthesis and fluorescence characteristics of novel asymmetric cyanine dyes for DNA detection. *J. Photochem. Photobiol. A* **2011**, *217*, 147–156. [[CrossRef](#)]
10. Soriano, E.; Holder, C.; Levitz, A.; Henary, M. Benz[c,d]indolium-containing monomethine cyanine dyes: Synthesis and photophysical properties. *Molecules* **2015**, *21*, 23. [[CrossRef](#)]
11. Kurutos, A.; Gadjev, N.; Deligeorgiev, T. Synthesis of novel asymmetric monomethine cyanine dyes containing benzoselenazolyl moiety. Fluorescent dsDNA probes. *Acta Sci. Nat.* **2015**, *2*, 90–98.
12. Fabijanić, I.; Kurutos, A.; Tomašić Paić, A.; Tadić, V.; Kamounah, F.S.; Horvat, L.; Brozovic, A.; Crnolatac, I.; Radić Stojković, M. Selenium-substituted monomethine cyanine dyes as selective G-quadruplex spectroscopic probes with theranostic potential. *Biomolecules* **2023**, *13*, 128. [[CrossRef](#)] [[PubMed](#)]
13. Saarnio, V.K.; Salorinne, K.; Ruokolainen, V.P.; Nilsson, J.R.; Tero, T.-R.; Oikarinen, S.; Wilhelmsson, L.M.; Lahtinen, T.M.; Marjomäki, V.S. Development of functionalized SYBR green II related cyanine dyes for viral RNA detection. *Dye. Pigment.* **2020**, *177*, 108282. [[CrossRef](#)]
14. Deligeorgiev, T.; Kaloyanova, S.; Vasilev, A. A novel general method for preparation of neutral monomethine cyanine dyes. *Dye. Pigment.* **2011**, *90*, 170–176. [[CrossRef](#)]
15. Alganatory, H.H.; Arief, M.M.H.; Amine, M.S.; Ebeid, E.-Z.M. Microwave-assisted solvent-free synthesis and fluorescence spectral characteristics of some monomethine cyanine dyes. *J. Chem. Pharm. Res.* **2014**, *6*, 143–161.
16. Deligeorgiev, T.G.; Gadjev, N.I.; Drexhage, K.-H.; Sabnis, R.W. Preparation of intercalating dye thiazole orange and derivatives. *Dye. Pigment.* **1995**, *29*, 315–322. [[CrossRef](#)]
17. Deligeorgiev, T.G.; Zaneva, D.A.; Katerinopoulos, H.E.; Kolev, V.N. A novel method for the preparation of monomethine cyanine dyes. *Dye. Pigment.* **1999**, *41*, 49–54. [[CrossRef](#)]
18. Gadjev, N.I.; Deligeorgiev, T.G.; Kim, S.H. Preparation of monomethine cyanine dyes as noncovalent labels for nucleic acids. *Dye. Pigment.* **1999**, *40*, 181–186. [[CrossRef](#)]
19. Deligeorgiev, T.; Vasilev, A.; Drexhage, K.-H. Synthesis of novel monomeric cyanine dyes containing 2-hydroxypropyl and 3-chloro-2-hydroxypropyl substituents—noncovalent labels for nucleic acids. *Dye. Pigment.* **2007**, *73*, 69–75. [[CrossRef](#)]
20. Deligeorgiev, T.; Vasilev, A.; Tsvetkova, T.; Drexhage, K.-H. Synthesis of novel monomeric asymmetric tri- and tetracationic monomethine cyanine dyes as fluorescent non-covalent nucleic acid labels. *Dye. Pigment.* **2007**, *75*, 658–663. [[CrossRef](#)]
21. Deligeorgiev, T.; Vasilev, A.; Drexhage, K.-H. Synthesis of novel cyanine dyes containing carbamoyl ethyl component—Noncovalent labels for nucleic acids detection. *Dye. Pigment.* **2007**, *74*, 320–328. [[CrossRef](#)]
22. Alfieri, M.L.; Panzella, L.; d’Ischia, M.; Napolitano, A. Bioinspired heterocyclic partnership in a cyanine-type acidichromic chromophore. *Molecules* **2020**, *25*, 3817. [[CrossRef](#)]

23. Eissa, F.M.; Abdel Hameed, R.S. Efficient green synthesis of monomethine cyanines via grinding under solvent-free conditions. *Green Process Synth.* **2016**, *5*, 283–288. [[CrossRef](#)]
24. Fei, X.; Yang, S.; Zhang, B.; Liu, Z.; Gu, Y. Solid-phase synthesis and modification of thiazole orange and its derivatives and their spectral properties. *J. Comb. Chem.* **2007**, *9*, 943–950. [[CrossRef](#)]
25. Deligeorgiev, T.G.; Gadjev, N.I.; Timtcheva, I.I.; Maximova, V.A.; Katerinopoulos, H.E.; Foukaraki, E. Synthesis of homodimeric monomethine cyanine dyes as noncovalent nucleic acid labels and their absorption and fluorescence spectral characteristics. *Dye. Pigment.* **2000**, *44*, 131–136. [[CrossRef](#)]
26. Alganzory, H.H.; El-Sayed, W.A.; Arief, M.H.; Amine, M.S.; Ebeid, E.M. Microwave synthesis and fluorescence properties of homo- and heterodimeric monomethine cyanine dyes TOTO and their precursors. *Green Chem. Lett. Rev.* **2017**, *10*, 10–22. [[CrossRef](#)]
27. Mikulin, I.; Ljubić, I.; Piantanida, I.; Vasilev, A.; Mondeshki, M.; Kandinska, M.; Uzelac, L.; Martin-Kleiner, I.; Kralj, M.; Tumir, L.-M. Polycationic monomeric and homodimeric asymmetric monomethine cyanine dyes with hydroxypropyl functionality—Strong affinity nucleic acids binders. *Biomolecules* **2021**, *11*, 1075. [[CrossRef](#)]
28. Tredwell, C.J.; Keary, C.M. Picosecond time resolved fluorescence lifetimes of the polymethine and related dyes. *Chem. Phys.* **1979**, *43*, 307–316. [[CrossRef](#)]
29. Åberg, U.; Åkesson, E.; Sundström, V. Excited state dynamics of barrierless isomerization in solution. *Chem. Phys. Lett.* **1993**, *215*, 388–394. [[CrossRef](#)]
30. Åberg, U.; Åkesson, E.; Alvarez, J.-L.; Fedchenia, I.; Sundström, V. Femtosecond spectral evolution monitoring the bond-twisting event in barrierless isomerization in solution. *Chem. Phys.* **1994**, *183*, 269–288. [[CrossRef](#)]
31. Sahyun, M.R.V.; Blair, J.T. Photophysics of a “simple” cyanide dye. *J. Photochem. Photobiol. A Chem.* **1997**, *104*, 179–187. [[CrossRef](#)]
32. Dietzek, B.; Yartsev, A.; Tarnovsky, A.N. Watching ultrafast barrierless excited-state isomerization of pseudocyanine in real time. *J. Phys. Chem. B* **2007**, *111*, 4520–4526. [[CrossRef](#)] [[PubMed](#)]
33. Weigel, A.; Pfaffe, M.; Sajadi, M.; Mahrwald, R.; Improta, R.; Barone, V.; Polli, D.; Cerullo, G.; Ernstring, N.P.; Santoro, F. Barrierless photoisomerisation of the “simplest cyanine”: Joining computational and femtosecond optical spectroscopies to trace the full reaction path. *Phys. Chem. Chem. Phys.* **2012**, *14*, 13350–13364. [[CrossRef](#)] [[PubMed](#)]
34. Piontkowski, Z.; Mark, D.J.; Bedics, M.A.; Sabatini, R.P.; Mark, M.F.; Detty, M.R.; McCamant, D.W. Excited state torsional processes in chalcogenopyrylium monomethine dyes. *J. Phys. Chem. A* **2019**, *123*, 8807–8822. [[CrossRef](#)]
35. Fürstenberg, A.; Vauthey, E. Ultrafast excited-state dynamics of oxazole yellow DNA intercalators. *J. Phys. Chem. B* **2007**, *111*, 12610–12620. [[CrossRef](#)]
36. Karunakaran, V.; Lustres, J.L.P.; Zhao, L.; Ernstring, N.P.; Seitz, O. Large dynamic Stokes shift of DNA intercalation dye thiazole orange has contribution from a high-frequency mode. *J. Am. Chem. Soc.* **2006**, *128*, 2954–2962. [[CrossRef](#)]
37. Zhao, Z.; Cao, S.; Li, H.; Li, D.; He, Y.; Wang, X.; Chen, J.; Zhang, S.; Xu, J.; Knutson, J.R. Ultrafast excited-state dynamics of thiazole orange. *Chem. Phys.* **2022**, *553*, 111392. [[CrossRef](#)]
38. Olsen, S.; McKenzie, R.H. Conical intersections, charge localization, and photoisomerization pathway selection in a minimal model of a degenerate monomethine dye. *J. Chem. Phys.* **2009**, *131*, 234306. [[CrossRef](#)] [[PubMed](#)]
39. Herz, A.H. Aggregation of sensitizing dyes in solution and their adsorption onto silver halides. *Adv. Coll. Interf. Sci.* **1997**, *8*, 237–298. [[CrossRef](#)]
40. Shindy, H.A.; El-Maghraby, M.A.; Eissa, F.M. Solvatochromism and halochromism of some furo/pyrazole cyanine dyes. *Chem. Int.* **2021**, *7*, 39–52. [[CrossRef](#)]
41. Norden, B.; Tjerneld, F. Optical studies on complexes between DNA and pseudoisocyanine. *Biophys. Chem.* **1977**, *6*, 31–45. [[CrossRef](#)]
42. Rye, H.S.; Quesada, M.A.; Peck, K.; Mathies, R.A.; Glazer, A.N. High-sensitivity two-color detection of double-stranded DNA with a confocal fluorescence gel scanner using ethidium homodimer and thiazole orange. *Nucleic Acids Res.* **1991**, *19*, 327–333. [[CrossRef](#)]
43. Nygren, J.; Svanvik, N.; Kubista, M. The interactions between the fluorescent dye thiazole orange and DNA. *Biopolymers* **1998**, *46*, 39–51. [[CrossRef](#)]
44. Larsson, A.; Carlsson, C.; Jonsson, M. Characterization of the binding of YO to [poly(dA-dT)]₂ and [poly(dG-dC)]₂, and of the fluorescent properties of YO and YOYO complexed with the polynucleotides and double-stranded DNA. *Biopolymers* **1995**, *36*, 153–167. [[CrossRef](#)] [[PubMed](#)]
45. Eriksson, M.; Härdelin, M.; Larsson, A.; Bergenholtz, J.; Akerman, B. Binding of intercalating and groove-binding cyanine dyes to bacteriophage T5. *J. Phys. Chem. B* **2007**, *111*, 1139–1148. [[CrossRef](#)]
46. Rye, H.S.; Yue, S.; Wemmer, D.E.; Quesada, M.A.; Haugland, R.P.; Mathies, R.A.; Glazer, A.N. Stable fluorescent complexes of double-stranded DNA with bis-intercalating asymmetric cyanine dyes: Properties and applications. *Nucleic Acids Res.* **1992**, *20*, 2803–2812. [[CrossRef](#)]
47. Rodger, A.; Norden, B. *Circular Dichroism and Linear Dichroism*; Oxford University Press: New York, NY, USA, 1997; Volume 1, p. 160.
48. Šmidlehner, T.; Piantanida, I.; Pescitelli, G. Polarization spectroscopy methods in the determination of interactions of small molecules with nucleic acids—tutorial. *Beilstein J. Org. Chem.* **2018**, *14*, 84–105. [[CrossRef](#)] [[PubMed](#)]

49. Šmidlehner, T.; Koščak, M.; Božinović, K.; Majhen, D.; Schmuck, C.; Piantanida, I. Fluorimetric and CD recognition between various ds-DNA/RNA depends on a cyanine connectivity in cyanine-guanidiniocarbonyl-pyrrole conjugate. *Molecules* **2020**, *25*, 4470. [CrossRef]
50. Silva, G.L.; Ediz, V.; Yaron, D.; Armitage, B.A. Experimental and computational investigation of unsymmetrical cyanine dyes: Understanding torsionally responsive fluorogenic dyes. *J. Am. Chem. Soc.* **2007**, *129*, 5710–5718. [CrossRef]
51. Timcheva, I.; Maximova, V.; Deligeorgiev, T.; Zaneva, D.; Ivanov, I. New asymmetric monomethine cyanine dyes for nucleic-acid labeling: Absorption and fluorescence spectral characteristics. *J. Photochem. Photobiol. A Chem.* **2000**, *130*, 7–11. [CrossRef]
52. Carlsson, C.; Larsson, A.; Jonsson, M.; Albinsson, B.; Norden, B. Optical and photophysical properties of the oxazole yellow DNA probes YO and YOYO. *J. Phys. Chem.* **1994**, *98*, 10313–10321. [CrossRef]
53. Larsson, A.; Carlsson, C.; Jonsson, M.; Albinsson, B. Characterization of the binding of the fluorescent dyes YO and YOYO to DNA by polarized light spectroscopy. *J. Am. Chem. Soc.* **1994**, *116*, 8459–8465. [CrossRef]
54. Netzel, T.L.; Nafisi, K.; Zhao, M.; Lenhard, J.R.; Johnson, I. Base-content dependence of emission enhancements, quantum yields, and lifetimes for cyanine dyes bound to double-strand DNA: Photophysical properties of monomeric and bichromophoric DNA stains. *J. Phys. Chem.* **1995**, *99*, 17936–17947. [CrossRef]
55. Deligeorgiev, T.; Timcheva, I.; Maximova, V.; Gadjev, N.; Drexhage, K.-H. Fluorescence characteristics of variously charged asymmetric monomethine cyanine dyes in the presence of nucleic acids. *J. Fluor.* **2002**, *12*, 225–229. [CrossRef]
56. Vasilev, A.; Deligeorgiev, T.; Gadjev, N.; Drexhage, K.-H. Synthesis of novel monomeric and homodimeric cyanine dyes based on oxazolo[4,5-b]pyridinium and quinolinium end groups for nucleic acid detection. *Dye. Pigment.* **2005**, *66*, 135–142. [CrossRef]
57. Mikelsons, L.; Carra, C.; Shaw, M.; Schweitzer, C.; Scaiano, J.C. Experimental and theoretical study of the interaction of single-stranded DNA homopolymers and a monomethine cyanine dye: Nature of specific binding. *Photochem. Photobiol. Sci.* **2005**, *4*, 798–802. [CrossRef] [PubMed]
58. Timcheva, I.I.; Maximova, V.A.; Deligeorgiev, T.G.; Gadjev, N.I.; Sabnis, R.W.; Ivanov, I.G. Fluorescence spectral characteristics of novel asymmetric monomethine cyanine dyes in nucleic acid solutions. *FEBS Lett.* **1997**, *405*, 141–144. [CrossRef] [PubMed]
59. Mahmood, T.; Paul, A.; Ladame, S. Synthesis and spectroscopic and DNA-binding properties of fluorogenic acridine-containing cyanine dyes. *J. Org. Chem.* **2010**, *75*, 204–207. [CrossRef]
60. Yarmoluk, S.M.; Kovalska, V.B.; Kryvorotenko, D.V.; Baland, A.O.; Ogul'chansky, T.Y. Interaction of cyanine dyes with nucleic acids. XXV. Influence of affinity-modifying groups in the structure of benzothiazol-4-[2,6-dimethylpyridinium] dyes on the spectral properties of the dyes in the presence of nucleic acids. *Spectrochim. Acta Part A* **2001**, *57*, 1533–1540. [CrossRef] [PubMed]
61. Biver, T.; De Biasi, A.; Secco, F.; Venturini, M.; Yarmoluk, S. Cyanine dyes as intercalating agents: Kinetic and thermodynamic studies on the DNA/Cyan40 and DNA/CCyan2 systems. *Biophys. J.* **2005**, *89*, 374–383. [CrossRef]
62. Biver, T.; Pulzonetti, M.; Secco, F.; Venturini, M.; Yarmoluk, S. A kinetic analysis of cyanine selectivity: CCyan2 and Cyan40 intercalation into poly(dA-dT) x poly(dA-dT) and poly(dG-dC) x poly(dG-dC). *Arch. Biochem. Biophys.* **2006**, *451*, 103–111. [CrossRef]
63. Yarmoluk, S.M.; Lukashov, S.S.; Ogul'chansky, T.Y.; Losytskyy, M.Y.; Korniyushyna, O.S. Interaction of cyanine dyes with nucleic acids. XXI. Arguments for half-intercalation model of interaction. *Biopolymers (Biospectroscopy)* **2001**, *62*, 219–227. [CrossRef]
64. El-Shishtawy, R.M.; Asiri, A.M.; Basaif, S.A.; Sobahi, T.R. Synthesis of a new B-naphthothiazole monomethine cyanine dye for the detection of DNA in aqueous solution. *Spectrochim. Acta Part A* **2010**, *75*, 1605–1609. [CrossRef] [PubMed]
65. Deligeorgiev, T.G.; Gadjev, N.I.; Vasilev, A.A.; Maximova, V.A.; Timcheva, I.I.; Katerinopoulos, H.E.; Tsikalas, G.K. Synthesis and properties of novel asymmetric monomethine cyanine dyes as non-covalent labels for nucleic acids. *Dye. Pigment.* **2007**, *75*, 466–473. [CrossRef]
66. Glavas-Obrovac, L.; Piantanida, I.; Marczy, S.; Mašić, L.; Timcheva, I.I.; Deligeorgiev, T.G. Minor structural differences of monomethine cyanine derivatives yield strong variation in their interactions with DNA, RNA as well as on their in vitro antiproliferative activity. *Bioorg. Med. Chem.* **2009**, *17*, 4747–4755. [CrossRef] [PubMed]
67. Tuma, R.S.; Beaudet, M.P.; Jin, X.; Jones, L.J.; Cheung, C.Y.; Yue, S.; Singer, V.L. Characterization of SYBR Gold nucleic acid gel stain: A dye optimized for use with 300-nm ultraviolet transilluminators. *Anal. Biochem.* **1999**, *268*, 278–288. [CrossRef] [PubMed]
68. Williams, L.R. Staining nucleic acids and proteins in electrophoresis gels. *Biotech. Histochem.* **2001**, *76*, 127–132. [CrossRef] [PubMed]
69. Zipper, H.; Brunner, H.; Bernhagen, J.; Vitzthum, F. Investigations on DNA intercalation and surface binding by SYBR Green I, its structure determination and methodological implications. *Nucleic Acids Res.* **2004**, *32*, e103. [CrossRef] [PubMed]
70. Schweitzer, C.; Scaiano, J.C. Selective binding and local photophysics of the fluorescent cyanine dye PicoGreen in double-stranded and single-stranded DNA. *Phys. Chem. Chem. Phys.* **2003**, *5*, 4911–4917. [CrossRef]
71. Koba, M.; Szostek, A.; Konopa, J. Limitation of usage of PicoGreen dye in quantitative assays of double-stranded DNA in the presence of intercalating compounds. *Acta Biochim. Pol.* **2007**, *54*, 883–886. [CrossRef] [PubMed]
72. The Molecular Probes Handbook. Nucleic Acid Detection and Analysis—Chapter 8. Nucleic Acid Stains—Section 8.1. Available online: <https://www.thermofisher.com/ru/ru/home/references/molecular-probes-the-handbook/nucleic-acid-detection-and-genomics-technology/nucleic-acid-stains.html> (accessed on 28 March 2023).
73. Rengarajan, K.; Cristol, S.M.; Mehta, M.; Nickerson, J.M. Quantifying DNA concentrations using fluorometry: A comparison of fluorophores. *Mol. Vis.* **2002**, *8*, 416–421. Available online: <http://www.molvis.org/molvis/v8/a49> (accessed on 4 May 2023). [PubMed]

74. Kolbeck, P.J.; Vanderlinden, W.; Gemmecker, G.; Gebhardt, C.; Lehmann, M.; Lak, A.; Nicolaus, T.; Cordes, T.; Lipfert, J. Molecular structure, DNA binding mode, photophysical properties and recommendations for use of SYBR Gold. *Nucleic Acids Res.* **2021**, *49*, 5143–5158. [[CrossRef](#)] [[PubMed](#)]
75. Saarnio, V.K.; Alaranta, J.M.; Lahtinen, T.M. Systematic study of SYBR green chromophore reveals major improvement with one heteroatom difference. *J. Mater. Chem. B* **2021**, *9*, 3484–3488. [[CrossRef](#)] [[PubMed](#)]
76. Karlsson, H.J.; Lincoln, P.; Westman, G. Synthesis and DNA binding studies of a new asymmetric cyanine dye binding in the minor groove of [poly(dA-dT)]. *Bioorg. Med. Chem.* **2003**, *11*, 1035–1040. [[CrossRef](#)]
77. Karlsson, H.J.; Eriksson, M.; Perzon, E.; Akerman, B.; Lincoln, P.; Westman, G. Groove-binding unsymmetrical cyanine dyes for staining of DNA: Syntheses and characterization of the DNA-binding. *Nucleic Acids Res.* **2003**, *31*, 6227–6234. [[CrossRef](#)]
78. Eriksson, M.; Karlsson, H.J.; Westman, G.; Akerman, B. Groove-binding unsymmetrical cyanine dyes for staining of DNA: Dissociation rates in free solution and electrophoresis gels. *Nucleic Acids Res.* **2003**, *31*, 6235–6242. [[CrossRef](#)]
79. Karlsson, H.J.; Bergqvist, M.H.; Lincoln, P.; Westman, G. Syntheses and DNA-binding studies of a series of unsymmetrical cyanine dyes: Structural influence on the degree of minor groove binding to natural DNA. *Bioorg. Med. Chem.* **2004**, *12*, 2369–2384. [[CrossRef](#)]
80. Uno, K.; Sugimoto, N.; Sato, Y. N-aryl pyrido cyanine derivatives are nuclear and organelle DNA markers for two-photon and super-resolution imaging. *Nat. Commun.* **2021**, *12*, 2650. [[CrossRef](#)]
81. Cosa, G.; Focsaneanu, K.-S.; McLean, J.R.N.; McNamee, J.P.; Scaiano, J.C. Photophysical properties of fluorescent DNA-dyes bound to single- and double-stranded DNA in aqueous buffered solution. *Photochem. Photobiol.* **2001**, *73*, 585–599. [[CrossRef](#)]
82. Rye, H.S.; Glazer, A.N. Interaction of dimeric intercalating dyes with single-stranded DNA. *Nucleic Acids Res.* **1995**, *23*, 1215–1222. [[CrossRef](#)]
83. Hansen, L.F.; Jensen, L.K.; Jacobsen, J.P. Bis-intercalation of a homodimeric thiazole orange dye in DNA in symmetrical pyrimidine–pyrimidine–purine–purine oligonucleotides. *Nucleic Acids Res.* **1996**, *24*, 859–867. [[CrossRef](#)] [[PubMed](#)]
84. Spielmann, H.P.; Wemmer, D.E.; Jacobsen, J.P. Solution structure of a DNA complex with the fluorescent bis-intercalator TOTO determined by NMR spectroscopy. *Biochemistry* **1995**, *34*, 8542–8553. [[CrossRef](#)] [[PubMed](#)]
85. Johansen, F.; Jacobsen, J.P. ¹H NMR studies of the bis-intercalation of a homodimeric oxazole yellow dye in DNA oligonucleotides. *J. Biomol. Struct. Dynam.* **1998**, *16*, 205–222. [[CrossRef](#)] [[PubMed](#)]
86. Jacobsen, J.P.; Pedersen, J.B.; Hansen, L.F.; Wemmer, D.E. Site selective bis-intercalation of a homodimeric thiazole orange dye in DNA oligonucleotides. *Nucleic Acids Res.* **1995**, *23*, 753–760. [[CrossRef](#)] [[PubMed](#)]
87. Timtcheva, I.; Maximov, V.; Deligeorgiev, T.; Gadjev, N.; Drexhage, K.H.; Petkova, I. Homodimeric monomethine cyanine dyes as fluorescent probes of biopolymers. *J. Photochem. Photobiol. B Biol.* **2000**, *58*, 130–135. [[CrossRef](#)]
88. Rye, H.S.; Dabora, J.M.; Quesada, M.A.; Mathies, R.A.; Glazer, A.N. Fluorometric assay using dimeric dyes for double- and single-stranded DNA and RNA with picogram sensitivity. *Anal. Biochem.* **1993**, *208*, 144–150. [[CrossRef](#)]
89. Murade, C.U.; Subramaniam, V.; Otto, C.; Bennink, M.L. Interaction of oxazole yellow dyes with DNA studied with hybrid optical tweezers and fluorescence microscopy. *Biophys. J.* **2009**, *97*, 835–843. [[CrossRef](#)]
90. Reuter, M.; Dryden, D.T.F. The kinetics of YOYO-1 intercalation into single molecules of double-stranded DNA. *Biochem. Biophys. Res. Commun.* **2010**, *403*, 225–229. [[CrossRef](#)]
91. Furstenberg, A.; Deligeorgiev, T.G.; Gadjev, N.I.; Vasilev, A.A.; Vauthey, E. Structure—Fluorescence contrast relationship in cyanine DNA intercalators: Towards rational dye design. *Chem. Eur. J.* **2007**, *13*, 8600–8609. [[CrossRef](#)]
92. Ogul'chansky, T.Y.; Yashchuk, V.M.; Losytskiy, M.Y.; Kocheshev, I.O.; Yarmoluk, S.M. Interaction of cyanine dyes with nucleic acids. XVII. Towards an aggregation of cyanine dyes in solutions as a factor facilitating nucleic acid detection. *Spectrochim. Acta Part A* **2000**, *56*, 805–814. [[CrossRef](#)]
93. Norden, B. Linear and circular dichroism of polymeric pseudoisocyanine. *J. Phys. Chem.* **1977**, *81*, 151–159. [[CrossRef](#)]
94. Chiriboga, M.; Green, C.M.; Mathur, D.; Hastman, D.A.; Melinger, J.C.; Veneziano, R.; Medintz, I.L.; Díaz, S.A. Structural and optical variation of pseudoisocyanine aggregates nucleated on DNA substrates. *Methods Appl. Fluoresc.* **2023**, *11*, 014003. [[CrossRef](#)]
95. Ogul'chansky, T.Y.; Losytskiy, M.Y.; Kovalska, V.B.; Yashchuk, V.M.; Yarmoluk, S.M. Interactions of cyanine dyes with nucleic acids. XXIV. Aggregation of monomethine cyanine dyes in presence of DNA and its manifestation in absorption and fluorescence spectra. *Spectrochim. Acta Part A* **2001**, *57*, 1525–1532. [[CrossRef](#)]
96. Zhou, X.; Mandal, S.; Jiang, S.; Lin, S.; Yang, J.; Liu, Y.; Whitten, D.G.; Woodbury, N.W.; Yan, H. Efficient long-range, directional energy transfer through DNA templated dye aggregates. *J. Am. Chem. Soc.* **2019**, *141*, 8473–8481. [[CrossRef](#)] [[PubMed](#)]
97. Yarmoluk, S.; Kovalska, V.; Kocheshev, I. Influence of the aggregation of homo-N-mer cyanine dyes on the nucleic acids detection sensitivity. *J. Fluor.* **2002**, *12*, 155–157. [[CrossRef](#)]
98. Biver, T.; Garcia, B.; Leal, J.M.; Secco, F.; Turrani, E. Left-handed DNA: Intercalation of the cyanine thiazole orange and structural changes. A kinetic and thermodynamic approach. *Phys. Chem. Chem. Phys.* **2010**, *12*, 13309–13317. [[CrossRef](#)]
99. Monchaud, D.; Allain, C.; Teulade-Fichou, M.P. Thiazole orange: A useful probe for fluorescence sensing of G-quadruplex-ligand interactions. *Nucleosides Nucleotides Nucleic Acids* **2007**, *26*, 1585–1588. [[CrossRef](#)] [[PubMed](#)]
100. Lubitz, I.; Zikich, D.; Kotlyar, A. Specific high-affinity binding of thiazole orange to triplex and G-quadruplex DNA. *Biochemistry* **2010**, *49*, 3567–3574. [[CrossRef](#)]

101. Kovalska, V.B.; Losytskyy, M.Y.; Yarmoluk, S.M.; Lubitz, I.; Kotlyar, A.B. Mono and trimethine cyanines Cyan 40 and Cyan 2 as probes for highly selective fluorescent detection of non-canonical DNA structures. *J. Fluor.* **2011**, *21*, 221–230. [[CrossRef](#)]
102. Doynikova, A.N.; Vekshin, N.L. Fluorescent determination of micro-quantities of RNA using Hoechst 33258 and binase. *Anal. Biochem.* **2019**, *576*, 5–8. [[CrossRef](#)]
103. Wu, Y.; Liu, Y.; Lu, C.; Lei, S.; Li, J.; Du, G. Quantitation of RNA by a fluorometric method using the SYTO RNASelect stain. *Anal. Biochem.* **2020**, *606*, 113857. [[CrossRef](#)]
104. Yoshino, Y.; Sato, Y.; Nishizawa, S. Deep-red light-up signaling of benzo[c,d]indole–quinoline monomethine cyanine for imaging of nucleolar RNA in living cells and for sequence-selective RNA analysis. *Anal. Chem.* **2019**, *91*, 14254–14260. [[CrossRef](#)] [[PubMed](#)]
105. Sato, Y.; Igarashi, Y.; Suzuki, M.; Higuchi, K.; Nishizawa, S. Deep-red fluorogenic cyanine dyes carrying an amino group-terminated side chain for improved RNA detection and nucleolar RNA imaging. *RSC Adv.* **2021**, *11*, 35436–35439. [[CrossRef](#)]
106. Aristova, D.; Kosach, V.; Chernii, S.; Slominsky, Y.; Balanda, A.; Filonenko, V.; Yarmoluk, S.; Rotaru, A.; Gizem Özkan, H.; Mokhir, A.; et al. Monomethine cyanine probes for visualization of cellular RNA by fluorescence microscopy. *Methods Appl. Fluor.* **2021**, *9*, 045002. [[CrossRef](#)] [[PubMed](#)]
107. Kandinska, M.I.; Cheshmedzhieva, D.V.; Kostadinov, A.; Rusinov, K.; Rangelov, M.; Todorova, N.; Ilieva, S.; Ivanov, D.P.; Videva, V.; Lozanov, V.S.; et al. Tricationic asymmetric monomeric monomethine cyanine dyes with chlorine and trifluoromethyl functionality–fluorogenic nucleic acids probes. *J. Mol. Liq.* **2021**, *342*, 117501. [[CrossRef](#)]
108. Yarmoluk, S.M.; Kryvorotenko, D.V.; Balanda, A.O.; Losytskyy, M.Y.; Kovalska, V.B. Proteins and cyanine dyes. Part III. Synthesis and spectroscopic studies of benzothiazolo-4-[1,2,6-trimethylpyridinium] monomethine cyanine dyes for fluorescent detection of bovine serum albumin in solutions. *Dye. Pigment.* **2001**, *51*, 41–49. [[CrossRef](#)]
109. Berlepsch, H.; Brandenburg, E.; Koksche, B.; Bottcher, C. Peptide adsorption to cyanine dye aggregates revealed by cryo-transmission electron microscopy. *Langmuir* **2010**, *26*, 11452–11460. [[CrossRef](#)]
110. Slavnova, T.O.; Görner, H.; Chibisov, A.K. Cyanine-based J-aggregates as a chirality-sensing supramolecular system. *J. Phys. Chem. B.* **2011**, *115*, 3379–3384. [[CrossRef](#)]
111. Volkova, K.D.; Kovalska, V.B.; Balanda, A.O.; Vermeij, R.J.; Subramaniam, V.; Slominskii, Y.L.; Yarmoluk, S.M. Cyanine dye–protein interactions: Looking for fluorescent probes for amyloid structures. *J. Biochem. Biophys. Methods* **2007**, *70*, 727–733. [[CrossRef](#)]
112. Volkova, K.D.; Kovalska, V.B.; Balanda, A.O.; Losytskyy, M.Y.; Golub, A.G.; Vermeij, R.J.; Subramaniam, V.; Tolmachev, O.I.; Yarmoluk, S.M. Specific fluorescent detection of fibrillar α -synuclein using mono- and trimethine cyanine dyes. *Bioorg. Med. Chem.* **2008**, *16*, 1452–1459. [[CrossRef](#)]
113. Volkova, K.D.; Kovalska, V.B.; Segers-Nolten, G.M.; Veldhuis, G.; Subramaniam, V.; Yarmoluk, S.M. Explorations of the application of cyanine dyes for quantitative α -synuclein detection. *Biotech Histochem.* **2009**, *84*, 55–61. [[CrossRef](#)]
114. Volkova, K.D.; Kovalska, V.B.; Losytskyy, M.Y.; Veldhuis, G.; Segers-Nolten, G.M.J.; Tolmachev, O.I.; Subramaniam, V.; Yarmoluk, S.M. Studies of interaction between cyanine dye T-284 and fibrillar alpha-synuclein. *J. Fluor.* **2010**, *20*, 1267–1274. [[CrossRef](#)] [[PubMed](#)]
115. Zhytniakivska, O.; Tarabara, U.; Kurutos, A.; Vus, K.; Trusova, V.; Gorbenko, G. Interaction of novel monomethine cyanine dyes with proteins in native and amyloid states. *East Eur. J. Phys.* **2022**, *2*, 124–132. [[CrossRef](#)]
116. Vus, K.; Tarabara, U.; Balklava, Z.; Nerukh, D.; Stich, M.; Laguta, A.; Vodolazkaya, N.; Mchedlov-Petrosyan, N.O.; Farafonov, V.; Kriklya, N.; et al. Association of novel monomethine cyanine dyes with bacteriophage MS2: A fluorescence study. *J. Mol. Liq.* **2020**, *302*, 112569. [[CrossRef](#)]
117. Mudliar, N.H.; Dongre, P.M.; Singh, P.K. An efficient J-aggregate based fluorescence turn-on and ratiometric sensor for heparin. *Sens. Actuators B Chem.* **2019**, *301*, 127089. [[CrossRef](#)]
118. Fürstenberg, A.; Julliard, M.D.; Deligeorgiev, T.G.; Gadjev, N.I.; Vasilev, A.A.; Vauthey, E. Ultrafast excited-state dynamics of DNA fluorescent intercalators: New insight into the fluorescence enhancement mechanism. *J. Am. Chem. Soc.* **2006**, *128*, 7661–7669. [[CrossRef](#)]
119. Shimizu, M.; Sasaki, S.; Kinjo, M. Triplet fraction buildup effect of the DNA-YOYO complex studied with fluorescence correlation spectroscopy. *Anal. Biochem.* **2007**, *366*, 87–92. [[CrossRef](#)]
120. Shin, H.-S.; Okamoto, A.; Sako, Y.; Kim, S.W.; Kim, S.Y.; Pack, C.-G. Characterization of the triplet state of hybridization-sensitive DNA probe by using fluorescence correlation spectroscopy. *J. Phys. Chem. A* **2013**, *117*, 27–33. [[CrossRef](#)]
121. Iliina, K.; Henary, M. Cyanine dyes containing quinoline moieties: History, synthesis, optical properties, and applications. *Chem. Eur. J.* **2021**, *27*, 4230. [[CrossRef](#)]
122. Li, W.K.W.; Jellett, J.-F.; Dickie, P.M. DNA distributions in planktonic bacteria stained with TOTO or TO-PRO. *Limnol. Oceanogr.* **1995**, *40*, 1485–1495. [[CrossRef](#)]
123. Marie, D.; Vaultot, D.; Partensky, F. Application of the novel nucleic acid dyes YOYO-1, YO-PRO-1, and PicoGreen for flow cytometric analysis of marine prokaryotes. *Appl. Environ. Microbiol.* **1996**, *62*, 1649–1655. [[CrossRef](#)]
124. Lippe, R. Flow virometry: A powerful tool to functionally characterize viruses. *J. Virol.* **2018**, *92*, e01765-17. [[CrossRef](#)] [[PubMed](#)]
125. Higuchi, K.; Sato, Y.; Togashi, N.; Suzuki, M.; Yoshino, Y.; Nishizawa, S. Bright and light-up sensing of benzo[c,d]indole-oxazolopyridine cyanine dye for RNA and its application to highly sensitive imaging of nucleolar RNA in living cells. *ACS Omega* **2022**, *7*, 23744–23748. [[CrossRef](#)] [[PubMed](#)]

126. Hilal, H.; Taylor, J.A. Cyanine dyes for the detection of double stranded DNA. *J. Biochem. Biophys. Methods* **2008**, *70*, 1104–1108. [[CrossRef](#)] [[PubMed](#)]
127. Wang, R.-Y.; Gao, X.; Lu, Y.-T. A surfactant enhanced stopped-flow kinetic fluorimetric method for the determination of trace DNA. *Anal. Chim. Acta* **2005**, *538*, 151–158. [[CrossRef](#)]
128. Atanasova, M.; Yordanova, G.; Nenkova, R.; Ivanov, Y.; Godjevargova, T.; Dinev, D. Brewing yeast viability measured using a novel fluorescent dye and image cytometer. *Biotechnol. Biotechnol. Equip.* **2019**, *33*, 548–558. [[CrossRef](#)]
129. Hwang, G.T. Single-labeled oligonucleotides showing fluorescence changes upon hybridization with target nucleic acids. *Molecules* **2018**, *23*, 124. [[CrossRef](#)]
130. Asseline, U.; Chassignol, M.; Aubert, Y.; Roig, V. Detection of terminal mismatches on DNA duplexes with fluorescent oligonucleotides. *Org. Biomol. Chem.* **2006**, *4*, 1949–1957. [[CrossRef](#)]
131. Koehler, O.; Seitz, O. Thiazole orange as fluorescent universal base in peptide nucleic acids. *Chem. Commun.* **2003**, *23*, 2938–2939. [[CrossRef](#)]
132. Koehler, O.; Venkatrao, D.; Jarikote, D.V.; Seitz, O. Forced intercalation probes (FIT probes): Thiazole orange as a fluorescent base in peptide nucleic acids for homogeneous single-nucleotide-polymorphism detection. *Chem. Bio Chem.* **2005**, *6*, 69–77. [[CrossRef](#)]
133. Jarikote, D.V.; Krebs, N.; Tannert, S.; Roder, B.; Seitz, O. Exploring base-pair-specific optical properties of the DNA stain thiazole orange. *Chem. Eur. J.* **2007**, *13*, 300–310. [[CrossRef](#)]
134. Bethge, L.; Jarikote, D.V.; Seitz, O. New cyanine dyes as base surrogates in PNA: Forced intercalation probes (FIT-probes) for homogeneous SNP detection. *Bioorg. Med. Chem.* **2008**, *16*, 114–125. [[CrossRef](#)] [[PubMed](#)]
135. Van Orden, A.; Keller, R.A.; Patrick Ambrose, W. High-throughput flow cytometric DNA fragment sizing. *Anal. Chem.* **2000**, *72*, 37–41. [[CrossRef](#)] [[PubMed](#)]
136. Ma, Y.; Shortreed, M.R.; Yeung, E.S. High-throughput single-molecule spectroscopy in free solution. *Anal. Chem.* **2000**, *72*, 4640–4645. [[CrossRef](#)] [[PubMed](#)]
137. Ma, Y.; Shortreed, M.R.; Li, H.; Huang, W.; Yeung, E.S. Single-molecule immunoassay and DNA diagnosis. *Electrophoresis* **2001**, *22*, 421–426. [[CrossRef](#)] [[PubMed](#)]
138. Zarkov, A.; Vasilev, A.; Deligeorgiev, T.; Stoynov, S.; Nedelcheva-Veleva, M. Novel fluorescent dyes for single DNA molecule techniques. *Mol. Imaging* **2013**, *12*, 90–99. [[CrossRef](#)]
139. Lange, N.; Szlasa, W.; Saczko, J.; Chwiłkowska, A. Potential of cyanine derived dyes in photodynamic therapy. *Pharmaceutics* **2021**, *13*, 818. [[CrossRef](#)]
140. Guan, M.; Chu, G.; Jin, J.; Liu, C.; Cheng, L.; Guo, Y.; Deng, Z.; Wang, Y. A combined cyanine/carbomer gel enhanced photodynamic antimicrobial activity and wound healing. *Nanomaterials* **2022**, *12*, 2173. [[CrossRef](#)]

Disclaimer/Publisher’s Note: The statements, opinions and data contained in all publications are solely those of the individual author(s) and contributor(s) and not of MDPI and/or the editor(s). MDPI and/or the editor(s) disclaim responsibility for any injury to people or property resulting from any ideas, methods, instructions or products referred to in the content.